Alma Mater Studiorum - Università di Bologna

DOTTORATO DI RICERCA IN

SCIENZE BIOMEDICHE E NEUROMOTORIE

Ciclo 35

Settore Concorsuale: 06/D6 – NEUROLOGIA

Settore Scientifico Disciplinare: MED/26 - NEUROLOGIA

EVALUATION OF THE TRANSCRIPTOMIC RESPONSE OF AN ALZHEIMER'S DISEASE MURINE MODEL INDUCED AT DIFFERENT AGES: SEARCHING FOR PREDICTORS

Presentata da: Giulia Sita

Coordinatore Dottorato

Matilde Yong Follo

Supervisore

Pietro Cortelli

Co-supervisore

Patrizia Hrelia

Esame finale anno 2023

SUMMARY

ABSTRACT

Alzheimer's disease (AD) is a chronic, progressive neurodegenerative disease, characterized by the impairment of mnesic and cognitive functions, that represents the most frequent type of dementia in older people worldwide. Aging is the most important risk factor for the sporadic form of the pathology and it is associated to the progressive impairment of the proteostasis network. The endoplasmic reticulum (ER), the main cellular actor involved in proteostasis, appears significantly compromised in AD due to the accumulation of β-amyloid (Aβ) protein and phosphorylated-tau protein. Increasing proteins misfolding activates a specific cellular response known as Unfolded Protein response (UPR) which orchestrates the recovery of ER function.

The aim of the present study was to investigate the role of UPR and aging process in a murine model of AD induced by intracerebroventricular (i.c.v.) injection of $A\beta_{1-42}$ oligomers at 3 or 18 months. The oligomers injection in aged animals caused the increased of memory impairment, oxidative stress, and the depletion of glutathione reserve. Furthermore, the RNA-sequencing analysis was performed and the bioinformatic analysis showed the enrichment of several pathways involved in neurodegeneration and protein regulations. The following analysis highlighted the significant dysregulation of the three branches of the UPR, the protein kinase RNA-like ER kinase (PERK), inositol-requiring protein 1α (IRE1α) and activating transcription factor 6 (ATF-6). In turn, ER stress affected the PI3K/Akt/Gsk3β and MAPK/ERK pathways, highlighting Mapkapk5 as a potential marker of the neurodegenerative process, which regulation could lead to the definition of new pharmacological and neuroprotective strategies to counteract AD.

GRAPHICAL ABSTRACT

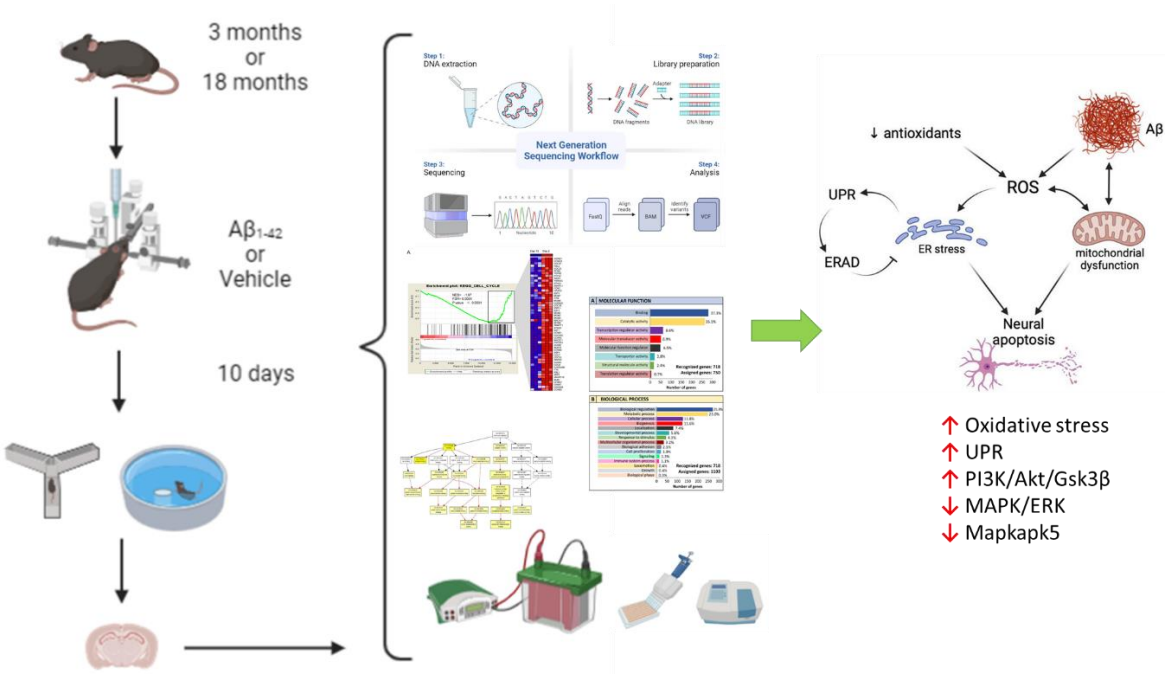

1. INTRODUCTION

Neurodegeneration defines a variety of conditions characterized by the progressive and consistent neuronal loss. Neurons are cells that form the central nervous system (CNS), and they are unable to reproduce or replace themselves. In this way, when damage threatens, the loss of cells will be permanent.

Clinical manifestations caused by neuronal damage are represented by mnesic alterations, motor difficulties, cognitive and behavioral disorders[1]. Several factors are involved in neuronal degeneration, beside environmental factors, genetic mutations and brain aging, also cellular and molecular events such as increase in oxidative stress, impaired mitochondrial functions, deposition of aggregated proteins, inflammatory response, activation of neuronal apoptosis, altered cell signaling and gene expression concur to the degenerative process[1].

Usually, patients are affected later in life and, with the consistent increase in life expectancy, in the last 20 years the number of diagnoses is prominently enhanced. These diseases are a central problem not only for patients but also for the entire health system[2]. Over the past decade, neurodegenerative diseases have been the subject of strong interest from all over the scientific world; however, so far, only palliative cares are available that are unable to slow or stop the progression of these pathologies. One crucial reason is represented by the fact that the diagnosis usually occurs late in the evolution of these pathology, when cellular death involves a great number of neurons[2].

In this view, the research for new biomolecular markers able to predict the insurgence of neurodegeneration and anticipating the diagnosis, could represent a critical step in the research for innovative therapeutic approach in the treatment of these devastating diseases.

1.1. Alzheimer's disease

Alzheimer's disease (AD) is a chronic and progressive neurodegenerative disease characterized by the impairment of cognitive functions. The disease was described for the first time by Dr. Alois Alzheimer in 1906 when he reported the case of Auguste Deter, a 51-year-old woman with behavioral changes, cognitive disturbance, disorientation, delusions, and diffuse brain atrophy[3].

AD begins 20 years or more before symptoms arise, with brain's alterations that are unnoticeable to the person affected[4]. Only after years of increasing brain changes, individuals experience noticeable symptoms may be observed[5]. These neuropathological features that characterized AD include the extracellular accumulation of toxic species of β-amyloid (Aβ) protein, in particular $A\beta_{1-40}$ and $A\beta_{1-42}$ to form amyloid plaques, the deposition of intracellular neurofibrillary tangles (NFT) of hyperphosphorylated tau protein, and neurodegeneration due to uncontrolled activation of microglia responsible for the secretion of neurotoxins and inflammatory factors[6,7].

In the first stages of the disease, patients may be asymptomatic or may exhibit various clinical manifestations from memory lapses to severe and debilitating loss of memory and cognitive function[5]. As AD progresses, neurons in other parts of the brain are damaged or destroyed and further neuropsychiatric symptoms may manifest, including confusion, disorientation, mood change, and eventually hallucination in later stages. Finally, basic bodily functions are affected, such as walking and swallowing, and patients become bed-bound and require 24 hours care until the death[8].

The physiological aging process involves slight cognitive deterioration too, for this reason it can often be difficult to distinguish cognitive decline due to AD from the declines associated with normal aging[9]. As a result of the complexity of the pathology, underdiagnosis is common and some evidences suggest that more than half of those who develop AD dementia may never be formally diagnosed[8,10].

Furthermore, there is an urgent need to develop new therapies for disease modification of AD and to address cognitive impairment and neuropsychiatric symptoms. According to the 2022 Alzheimer's disease drug development pipeline (Fig. 1), currently there are 143 agents in clinical trials and most drugs under evaluation aim to achieve disease modification by targeting the underlying

biological processes of AD[11]. However, for a novel disease-modifying therapy to be effective it has to be started years before of potentially irreversible pathologic changes have occurred, for this reason, identifying individuals destined to develop AD dementia is vital[12].

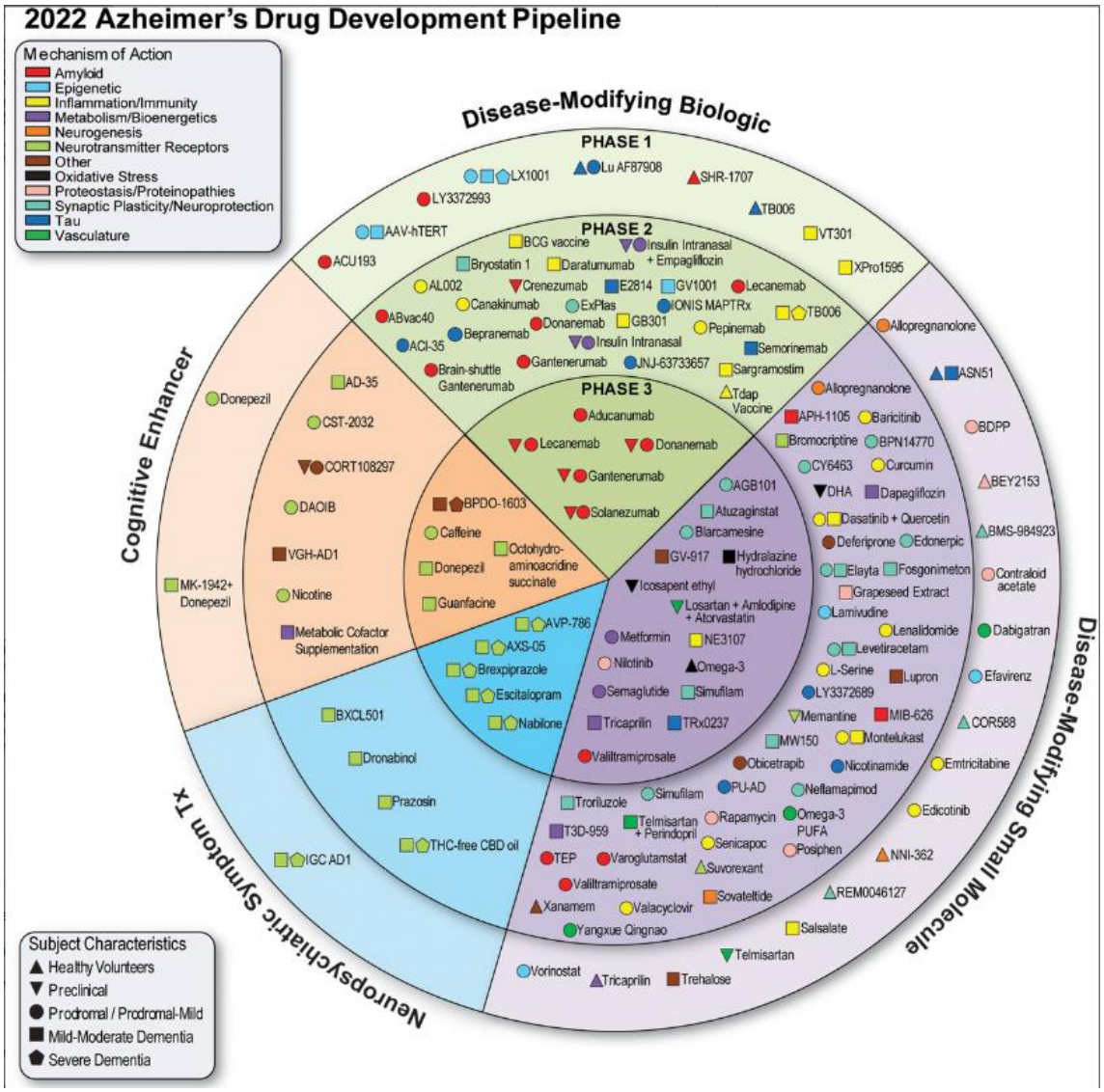

Figure 1. Agents in clinical trials for treatment of AD in 2021 (from clinicaltrials.gov as of the index date of January 5, 2021). The inner ring shows Phase 3 agents; the middle ring comprises Phase 2 agents; the outer ring presents Phase 1 therapies; agents in green areas are biologics; agents in purple are disease-modifying small molecules; agents in orange areas are symptomatic agents addressing cognitive enhancement or behavioral and neuropsychiatric symptoms; the shape of the icon shows the population of the trial; the icon color shows the Common Alzheimer's Disease Research Ontology (CADRO)-based class of the agent ("Other" category includes CADRO classes that have three or fewer agents in trials). Agents underlined are new to the pipeline since 2020.

1.1.1. Epidemiology

To date, the number of dementia patients is evaluated to reach 152 million before 2050, with the greatest increase expected in low-and middle-income countries[13]. Indeed,

the average age of population is constantly increasing, and the number of dementia's patients will increase too. AD is the leading cause of cognitive impairment and dementia worldwide affecting the 3-4% of adults after 65 years of age[7,14]. From 2000 to 2018 death tolls with AD increased 146.2% becoming the fifth-leading cause of death after 65 years old with 122,019 victims, and it may cause even more deaths than officially recognized[8,15]. AD is also a leading cause of disability and morbidity, thus, while recent findings are promising, the social and economic burden of AD will continue to be huge and unsustainable.

A growing number of studies indicate that the prevalence and incidence of AD and other dementias in the higher-income Western countries may have declined in the past 25 years[16–18] (Fig. 2).

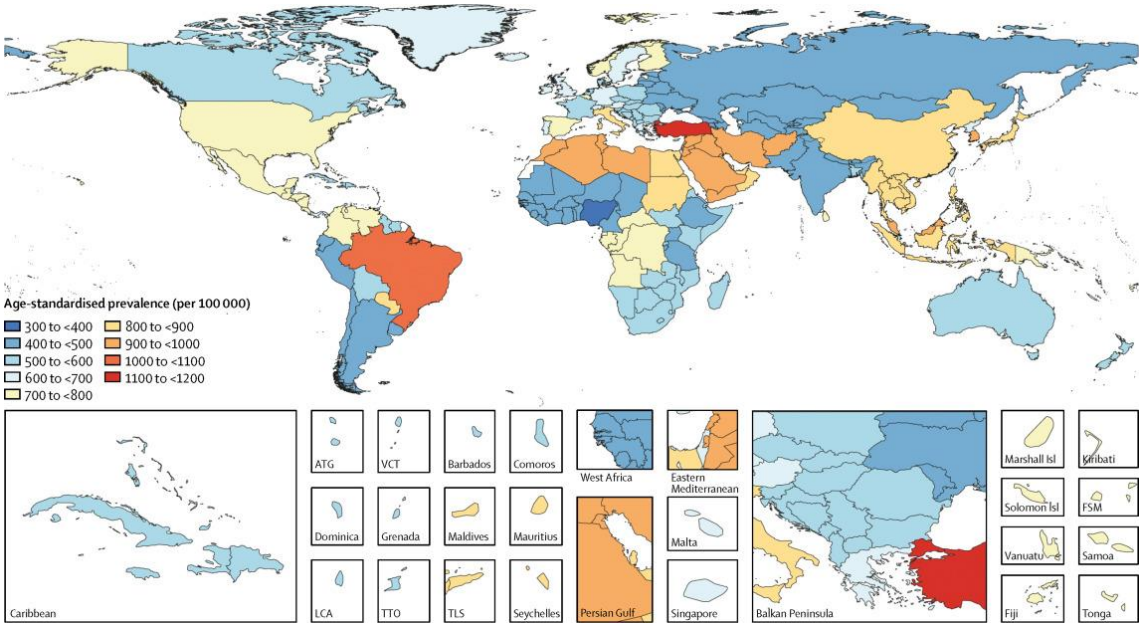

Figure 2. Age-standardised prevalence for Alzheimer's disease and other dementias per 100 000 population by location for both sexes, 2016. ATG=Antigua and Barbuda. FSM=Federated States of Micronesia. Isl=Islands. LCA=Saint Lucia. TLS=Timor-Leste. TTO=Trinidad and Tobago. VCT=Saint Vincent and the Grenadines.

These declines have been attributed to increasing levels of education and improved control of cardiovascular risk factors[19]. Such findings are promising and suggest that identifying and reducing risk factors for AD and other dementias may be effective. Although these findings indicate that a person's risk of dementia at any given age may be decreasing slightly, the total number of people with AD is expected to continue to increase dramatically consistent with the aging of the population[8]. Moreover, to date it is not possible to predict the effect of the increasing diagnosis of diabetes and obesity — potential risk factors for AD — which may lead to a rebound in dementia risk in coming

years[16]. On the contrary, 68% of the projected increase in the global prevalence and burden of dementia by 2050 will take place in low- and middle-income countries, where there is currently no evidence that the risk of AD has been declining[20].

In Europe, the incidence of AD rose with increasing age strata: 65–74 years, 3%; 75–84 years, 17%; > 85 years, 32%, and two times higher in women than in men[14]. Particularly, the age-standardized mortality rate of women is also higher than men, suggesting the longer life expectancy is not the only determinant of the women dominance[21]. Epidemiological investigations have provided robust evidence that behavioral and environmental factors have key roles in disease pathogenesis and progression. Especially, preexisting disease is more common in AD patients than others of the same age[22].

1.1.2. Pathophysiology of Alzheimer's disease

Extracellular Aβ plaques and intracellular NFT of tau protein are recognized hallmark of AD[23]. One of the most accepted theories about AD pathogenesis identifies the cerebral accumulation of Aβ peptide as the result of the imbalance between protein production and clearance, and the main event leading to a cascade consequences[24]. The Aβ peptide may have a different number of aminoacids (36 to 43) and is derived from the proteolysis of the amyloid precursor protein (APP), an important protein for the brain's homeostasis[25]. The APP may be processed by two different pathways, the non-amyloidogenic and the amyloidogenic. In the first case, APP is cleaved by α-secretase resulting in sAPPα, a molecule which probably has important roles in brain plasticity and neurons survival and protection[26]. In the amyloidogenic pathway APP is sequentially cleaved by β- and γ-secretases, the first products are a soluble product, sAPPβ, related to neuronal death, and a carboxy-terminal complex which is then cleaved to give Aβ peptide[27] (Fig. 3). In physiological conditions, the amyloidogenic and non-amyloidogenic pathways coexist in equilibrium and Aβ peptides are produced as monomers with synapses protective functions[28]. Although Aβ peptide may exist with different number of aminoacids, dependently to the site at which γ-secretases cleaves the protein chain, $A\beta_{1-40}$ and $A\beta_{1-42}$ are the most abundant forms[29]. The $A\beta_{1-40}$ is the most frequent, but $A\beta_{1-42}$ is more neurotoxic and prone to aggregation in fibrils that accumulate in Aβ plaques observed in AD patients.

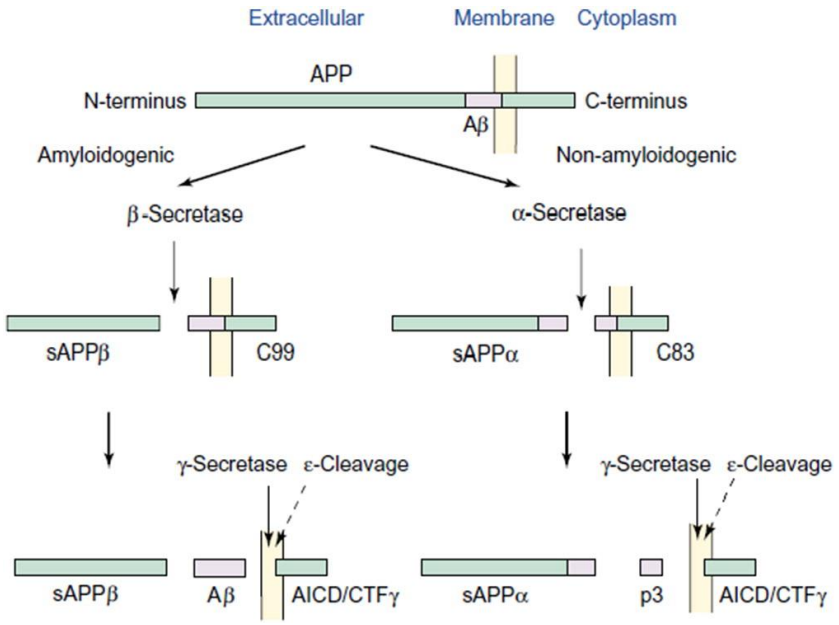

Figure 3. The structure and processing of APP showing amyloidogenic and non-amyloidogenic pathways. Aβ (purple box) constitutes part of the transmembrane domain and an adjacent short fragment of the extracellular domain.

Increased levels of Aβ peptide result in the formation of oligomers leading to neuronal toxicity and degeneration, interfering with the function and survival of cholinergic, serotonergic, noradrenergic and dopaminergic neurons, reducing their control over the amyloidogenic pathway and favoring the accumulation of insoluble Aβ peptide[30]. Indeed, soluble oligomeric Aβ seems to be the more neurotoxic species for their effects on synaptic plasticity[31].

The $A\beta_{1-42}$ aggregates and blocks both glutamate receptor α-amino-3-hydroxy-5-methyl-4-isoxazolepropionic acid (AMPA) and calcium (Ca^{2+}) channels increasing its intracellular concentration[32]. These events and the increasing local inflammatory response induce apoptosis, triggering neuronal cells to death[33,34]. Furthermore, during the aggregation phase, Aβ produces hydrogen peroxide (H_2O_2) which induce reactive oxygen species (ROS) formation responsible for the lipid peroxidation of cellular membranes, and for the consequent disturbance of cellular homeostasis and metabolism, making neurons susceptible to apoptosis[33].

The Aβ deposition precedes NFT formation, but the mechanism by which Aβ peptide promotes hyperphosphorylation of tau protein is still unclear. Tau protein is a structural protein associated with the cytoskeleton of neurons, its misfolding and the consequent formation of NFT leads to neuronal damage, promotes cytotoxicity, and finally triggers cells to death[35,36]. In 2006 Blurton Jones & LaFerla suggested multiple mechanisms, the Aβ peptide may promote the activation of specific kinases as glycogen

synthase kinase 3β (GSK3β) that catalyze the hyperphosphorylation of tau protein; through the neuroinflammatory response induced by Aβ deposition; the deregulation of the degradation of tau protein; and the inadequate localization of tau protein caused by defects in axonal transport which can lead to hyperphosphorylation and aggregation in NFT[37] (Fig. 4).

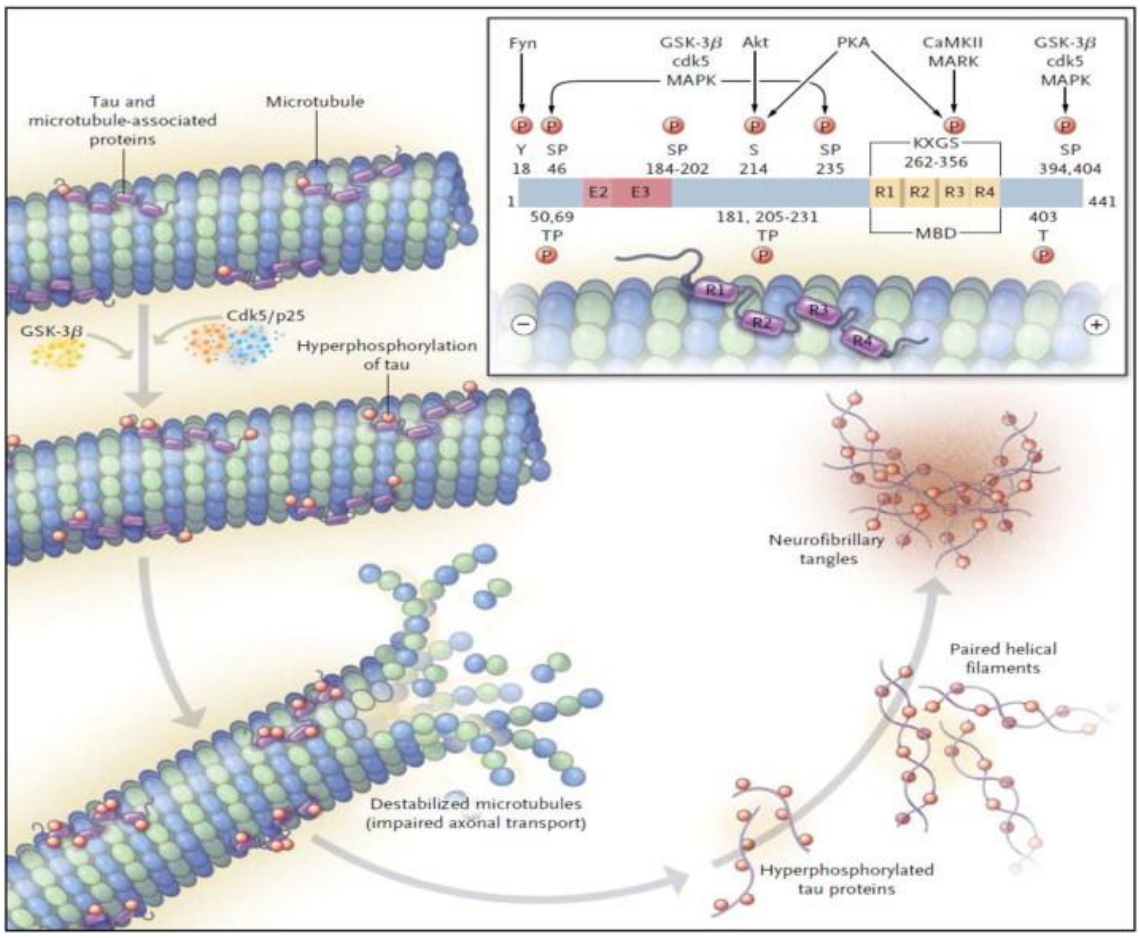

Figure 4. Showing structure of microtubule binding domain of tau protein with phosphorylation sites (Inset). The hyperphosphorylation of tau by GSK3β, cyclin-dependent kinase (cdk5) resulted into destabilization microtubules followed by detachment of tau and self-aggregation into paired helical filament.

The $A\beta_{1-42}$ is initially found at higher concentrations in the amyloid plaques observed in AD patients[38]. Several studies showed that in the cerebrospinal fluid (CSF) $A\beta_{1-42}$ levels are markers of underlying brain amyloidosis but these levels decrease in AD patients, probably due to the higher deposition of Aβ plaques[39]. Another evidence of the involvement of $A\beta_{1-42}$ peptide in the AD pathophysiology, is that mutations in APP and presenilin genes, which give rise to early-onset familial AD forms, lead to a relative increase in peptide levels[38]. Although Aβ plaques and NFT are recognized biomarkers for AD, some individuals that have only these two biomarkers never develop cognitive

symptoms[40]. This condition makes even more difficult to obtain a pre-symptomatic diagnosis.

Experimental models are essential to understand AD pathogenesis and to perform preclinical testing of novel therapeutics. To date, the vast majority of experimental models are transgenic mice that express human genes that result in the formation of amyloid plaques and neurofibrillary tangles[41]. According to our current knowledge, there is still no animal model with all the cognitive, behavioral, biochemical and histopathological abnormalities that characterize AD. The published studies have demonstrated that i.c.v. injection with $A\beta_{1-42}$ to mice could induce significant neuron death, inflammatory response and memory impairments[42]. Indeed, a rising concentration of Aβ in the brain is a critical factor in the development of late-onset sporadic AD, playing a key role in triggering the "amyloid cascade." Although transgenic models, such as APP- and PS-1-overexpressing models are known to be useful in the study of genetic aspects of early-onset AD, the sporadic form of the disease, that accounts for approximately 90% of all cases, requires unique approaches to model this form of AD[43]. Growing evidence indicates that Aβ-injected rodent models of AD might closely mimic the main neuropathological symptoms present in AD patients when concentrations of Aβ are increasing[43]. Many studies have reported behavioral and neurochemical consequences obtained after i.c.v. injection of the $A\beta_{1-42}$ peptide. In these studies, the most widely used dose is 400 pmol, but a much lower dose (240 pmol) will allow to assess the early effects of Aβ oligomers. Moreover, 200 pg of Aβ peptide is the approximate quantity of the protein in a single amyloid plaque in AD brain[44].

1.1.3. Risk factors

Although a great effort has been spent to comprehend the etiopathology of AD, to date is not possible to define a clear and specific mechanism responsible for its onset. Indeed, AD is a complex, multifactorial disease in which several factors are involved. Similarly, a plethora of risk factors have been identified, some of them not modifiable and other modifiable, mostly related to the individual lifestyle.

Among not modifiable risk factors, the genetic signature has a prevalent role. Genetic is the most important risk factor for early-onset AD which affects individuals under 65 years of age and accounting for about 4-6% of cases of disease[27]. According to Ballard et al. about 70% of the risk of developing AD can be attributed to genetics[45]. Several genes have been identified as causal and many other as possible risk factors. Early

onset AD is frequently associated to the mutations of presenilin-1 (PSEN1, 80% of the cases) or PSEN2 (5% of the cases) and APP (15% of the cases)[46]. In physiological conditions, PSEN1 and PSEN2 encode for two subcomponents of γ-secretase. Mutant PSEN1 may reduce the γ-secretase activity and enhance 42-specific-γ-secretase cleavage of normal APP which lead to an increase of $A\beta_{1-42}$:$A\beta_{1-40}$ ratio and to Aβ deposition[47,48]. Moreover, PSEN1 and PSEN2 may be involved in many other cellular mechanisms not related to the APP metabolism as notch signaling, calcium homeostasis, gene expression and neuroprotective functions[49–52]. The APP is a transmembrane protein widely expressed in all cells, although its physiological function is not fully understood yet, increasing evidence suggests an important role in the regulation of neurons' survival[53]. Thirty mutations have been found in the APP gene, all of them near to the secretase cleavage site and causing an increase in the $A\beta_{1-42}/A\beta_{1-40}$ ratio and of Aβ plaques in the hippocampus and cortex[54].

Also, in the late onset of AD (LOAD) several genes maybe associated to an elevated risk of AD. In particular, the presence of the allele 4 for apolipoprotein E (APOE4) increases the risk of acquiring LOAD[55]. The ApoE protein is a glycoprotein highly expressed in astrocytes and microglia involved in lipid metabolism, like cholesterol essential for myelin production and normal brain function[56]. Several studies have underlined the role, as risk factors for AD, for the genes involved in cholesterol transport suggesting deterioration of cholesterol homeostasis[57]. The presence of ε4 allele in heterozygosity increases 3-fold the risk of AD developing, whereas in homozygosis, the risk is increased 12-fold[58]. Indeed, ApoEε4 promotes the formation of Aβ fibrils and their deposition in plaques accelerating the development of the disease[55]. On the contrary, the presence of ε2 and ε3 alleles reduce the risk of AD promoting the clearance of Aβ peptide[58].

Beyond APOE, clusterin (CLU) has been recently recognized as a risk factor for LOAD. Indeed, the CLU is upregulated not only in the hippocampus and in the cortex of AD's patients, but also in plasma and CSF. However, its role as neurotoxic, reducing the clearance of Aβ, or as neuroprotector, promoting the clearance, is poorly understood yet[59].

Beside the genetic contributions to AD, also age, previous head injury and hypertension have been identified as risk factors[60]. Furthermore, several conditions, as cardiovascular and cerebrovascular diseases, diabetes mellitus, obesity, high cholesterol level, and smoking have been identified as probable risk factors that could lead to AD[61].

The physiological aging process is the most important risk factor for LOAD[62]. Indeed, the prevalence of AD is around 19% in individuals 75-84 years of age and increases to 30-35% for those older than 85 years[63]. Moreover, the consideration that AD could be viewed as an accelerated form of normal aging is largely due to the observation that many of the pathological changes identified in AD are similar, but more severe, to those that characterized normal aging, as the reduction of the brain volume and weight, the synapses' loss, and the formation of Aβ plaques and NFT[64].

Several studies have highlighted an history of traumatic brain injuries (TBI) in AD patients[65,66]. TBI could cause the damage of the blood-brain barrier (BBB) with the result of a leakage of plasma protein and an increase of neuroinflammatory response. Moreover, after a TBI is possible to observe an increase of APP, leading to the deposition of Aβ, probably as an acute-phase response to neuronal injury[67]. Promisingly, statins as the rosuvastatin, owing to the potential neuroprotective effects, might reduce the dementia risk after TBI[68].

Another recognized risk factor for AD is hypertension in middle age which could cause changes in vessels walls leading to hypoperfusion, dysfunction of the BBB, hypoxia and ischemia that, in turn, leads to the accumulation of APP and Aβ, and to the expression of PSEN contributing to AD development[69]. Furthermore, the integrity of the vascular system is essential for normal brain functions and all the changes may precede and contribute to the cognitive decline and to AD[70]. Vascular injury leads to increased expression of APP and Aβ peptide formation, whose clearance is decreased by BBB dysfunction. In addition, BBB leakage leads to oligoemia and to accumulation of neurotoxic molecules, causing neuronal damage. The accumulation of Aβ amplifies neuronal dysfunction contributing to the neurodegenerative process. Finally, both Aβ peptide accumulation and hypoperfusion lead to the hyperphosphorylation of tau protein, promoting the formation of NFT[71].

Epidemiological studies suggest an association between type 2 diabetes mellitus and the increased risk to develop AD[72]. Indeed, deficiency or resistance to insulin induce the activity of β- and γ-secretases, which in turn lead to the accumulation of Aβ protein also reducing its clearance[27]. Furthermore, insulin resistance or deficiency are still capable of inducing hyperphosphorylation of tau protein, leading to NFT formation through the abnormal activation of GSK3β[73]. Diabetics patients not properly treated show an increase of the level of p-tau in the CSF than those using antidiabetic drugs, suggesting that tau pathology might be ameliorated with the antidiabetic drugs[74].

Finally, another modifiable risk factor in the development of AD is smoking, due to its ability to raise the generation of free radicals increasing oxidative stress, and to promote pro-inflammatory factors leading to the activation of phagocytes, and as a consequence, to oxidative damage. Furthermore, smoking may lead to cerebrovascular disease, which increase the risk of AD[75].

In conclusion, modifiable risk factors such as diabetes, hypertension and dyslipidemia and others previously mentioned should be closely monitored to prevent complications favoring cognitive decline or even to improve the quality of life of patients with AD. Since no current drug intervention can modify the pathophysiological mechanisms related to the development of this devastating disease, adoption of these measures constitutes an important strategy for clinical management in order to prevent or postpone cognitive decline.

1.2. Aging and Alzheimer's disease

Aging is the time-dependent physiological functional decline that is also the most important risk factor for many diseases, including AD. Considering the rate at which the human population is aging, it becomes imperative to identify means by which to maintain cognitive integrity by protecting against, or even counteracting, the effects of aging. Indeed, due to the growing aging population and the increased burden of health care for people with AD, the research on this disease is rapidly expanding. Given the fact that AD is one of the best-known aging-linked disease, it will be interesting to understand how AD and aging are intrinsically linked, and how the research in the two fields could impact and inspire each other, at the molecular, cellular, and system level[76].

A significant difference between aging and AD is that the number of neurons does not change very much during aging, but neuron and synapse loss are hallmarks of AD. Moreover, the proinflammatory and oxidative environment promoted by aging, is much more exacerbated in AD, and chronic inflammation seems to be a common feature between aging and AD[76].

1.2.1. Neuroinflammation

Neuroinflammation generally refers to an inflammatory response within the CNS that can be caused by various pathological insults, including infection, trauma, ischemia and toxins[77]. The process is marked by the production of pro-inflammatory cytokines,

including IL-1β, IL-6, IL-18 and tumor necrosis factor (TNF), chemokines, and ROS by innate immune cells in the CNS[77]. The release of pro-inflammatory molecules lead to synaptic dysfunction, neuronal death and inhibition of neurogenesis[78]. However, although anti-inflammatory cytokines are produced to prevent an extensive inflammatory response, in the context of neurodegenerative disease, neuroinflammation is a chronic process that fails to resolve by itself and is considered a driver of the disease.

AD is a multifaced disease in which several pathological processes are involved beside the extracellular depositions of Aβ plaques and the intracellular accumulation of NFT. Indeed, also inflammation plays a crucial role in AD onset and evolution, as confirmed by the presence of elevated levels of inflammatory markers in patients as well as of AD risk genes associated with immune functions[79].

Microglia are the principal immune cells in the CNS, where they support neurons and respond to stimuli[80]. Historically microglia has been characterized by two states, the resting state during which they surveil neuronal parenchyma with ramified processes, and a reactive state that allows a morphological change to provide additional defense and restoration of tissue homeostasis[81]. In the mature healthy CNS, the distribution of microglia is largely uniform and the cell bodies are largely sessile, but their processes are constantly moving and scanning the brain parenchyma[82].

It is now clear that microglia exist in diverse, dynamic, and multidimensional states depending on the context, including local environment[83] (Fig. 5).

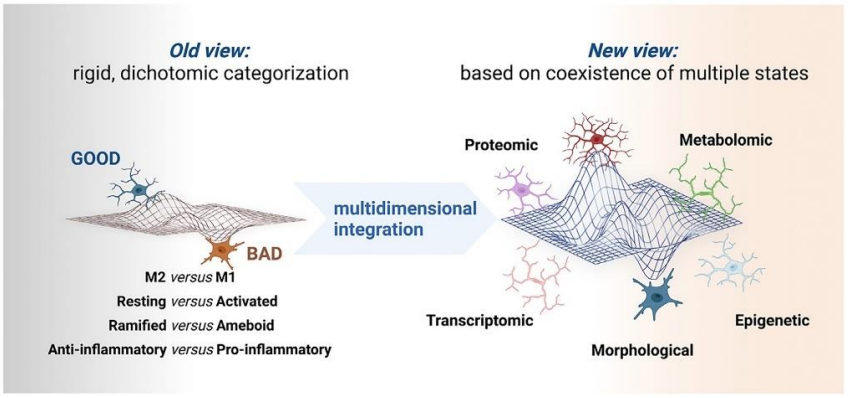

Figure 5. Microglia have been traditionally framed into dichotomic categories, but our current integration of epigenetic, transcriptomic, metabolomic, and proteomic data favors a multidimensional integration of coexisting states.

Microglia have a complex "sensome,"[84] a series of surface receptors that allow them to detect changes in their environment. Microglial states are thus dynamic, and the outcome of the cell's epigenome, transcriptome, proteome, and metabolome yields discrete morphological, ultrastructural, and functional outputs[83].

The term “homeostatic” is used to refer to microglia in physiological conditions, but there are different interpretations of this nomenclature when describing microglia in health and disease. While homeostatic relates to the “physiological” context, it does not necessarily correspond to a unique molecular profile because, even without any perturbation, microglia display diverse morphological and functional states depending on the signals from the CNS microenvironment. A less responsive microglial state, which in other contexts would be considered more homeostatic, might be less effective at responding to damage or pathological cues in aging and disease contexts. For example, during aging these cells show changes in density, morphology, and cytokine expression resulting in a persistent inflammatory environment known as “inflammaging”, which in turn makes the CNS more susceptible to injury or neurodegeneration[85]. Indeed, in aging and neurodegenerative disease, microglia may have reduced ability to rapidly respond to brain challenges (i.e., removing toxic amyloid, infected, damaged, or degenerating neurons), leading to CNS dysfunction and disease progression. Microglia from adult TREM2 knockout mice have been described as “locked in a homeostatic state” as they are less responsive to Aβ and do not adopt a disease-associated microglia (DAMs) signature in disease contexts[86]. From this example, the term “homeostatic” is not informative if not well defined and placed in the context of function.

DAM signature includes downregulation of CX3CR1 and P2RY12 and upregulation of APOE, AXL, SPP1, and TREM2[87]. Several studies, in both mouse and human stem-cell-differentiated microglia, demonstrated that the transition to a DAM state is dependent on TREM2[88]. How the TREM2 receptor drives the DAM transcriptional phenotype remains unclear, although the TREM2-ApoE signaling pathway is necessary for the switch from homeostatic to the microglial neurodegenerative phenotype[88]. Further investigations are required to fully elucidate the role of TREM2.

New bulk and single-cell epigenetic approaches may provide a means to switch microglial states at will, enabling the field to finally understand the function of distinct microglial states and their impact in different contexts. Additionally, many genes of the DAM signature were identified across various contexts. For example, a common set of markers including an upregulation of TREM2, APOE, CD11c, CLEC7A, and LPL and downregulation of TGFβ, CSF1R, P2RY12, and TMEM119 has been recently used to denote a microglial state that associates with myelinating areas in the developing brain but also with aging and several models of degenerative diseases, such as AD[89]. These observations raise the question as to whether the DAM is a signature strictly associated

with certain diseases, or represents a response to various challenges and may differ between the young/developing versus aged/diseased CNS and across distinct regions. Most likely, the same states that are beneficial in certain contexts may be detrimental in others, strictly depending on the complex interactions between microglia and their surrounding environment.

Furthermore, activated microglia stimulate neurons to overproduce Aβ, resulting in synaptic loss, the formation of extracellular plaques, and subsequent NFT formation[90]. These effects, in turn, promote increased microglial activation creating a positive feedback loop that drives the development of AD[91]. Indeed, initially microglial activation may serve to eliminate Aβ, but their chronic activation may amplify the amyloid cascade leading to neurotoxicity[92].

Also astrocytes, the most abundant cell type in the CNS play a fundamental role in the regulation of neurons' maturation helping to maintain their functions[93]. Astrocytes may act as neuroprotectors reducing inflammation and stimulating repair, or driving neurotoxicity promoting inflammation[94]. They respond to inflammatory molecules such as cytokines and chemokines and are able to detect aggregated proteins such as Aβ[93]. In aging, astrocytes change in number, morphology, and show increased oxidative damage and enhanced superoxide production together with increased production of pro-inflammatory cytokines[95]. This phenotype, in turn, can be triggered by different stimuli including oxidative stress, inflammation and inhibition of the ubiquitin-proteasome system, and has been implicated in the pathogenesis of neurodegenerative disease, as AD[96]. Astrocyte senescence has been implicated in the pathogenesis of neurodegenerative diseases[97].

Neuroinflammation and oxidative stress are key pathologic signatures of AD[98]. ROS are produced by all aerobic cells, and while they are essential signaling molecules, a redox imbalance is detrimental and plays an important role in the inflammatory process in aging as well as in AD[99]. While cells of innate immunity produce copious amounts of ROS within the CNS, it is not clear whether neuroinflammation induces oxidative stress or if it is the elevated levels of ROS that cause neuroinflammation, especially in a situation where there is already excess oxidant production and a reduction of antioxidant defense[77]. Thus, the chronic inflammatory environment raises oxidative stress, which then increases homeostasis's loss, particularly involving the regulatory systems and the immune response, producing a vicious cycle. A recent study found that elevated levels of oxidative stress biomarkers are associated with high levels of inflammatory cytokines,

both of which are due to poor cognitive performance in elderly patients[100]. A vicious oxi-inflamm-aging cycle is thus created in aging and exaggerated in AD[101] (Fig. 6).

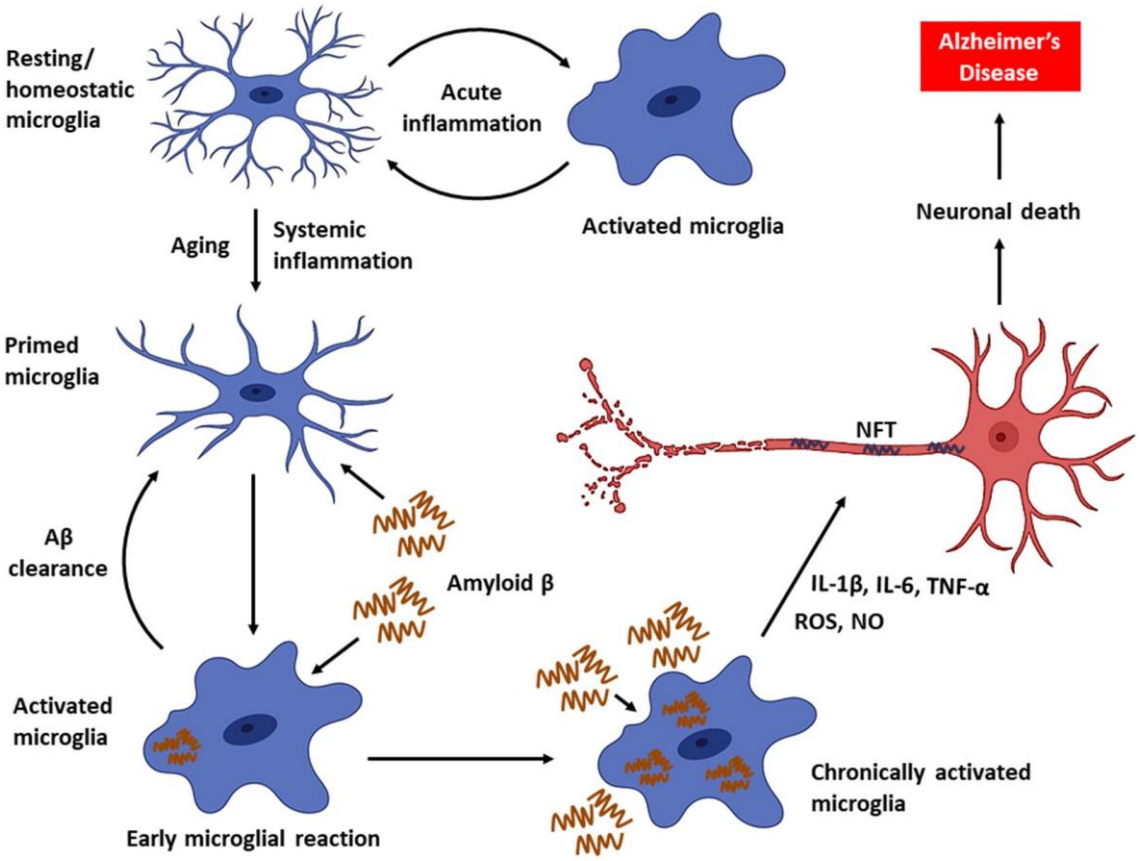

Figure 6. Microglial activity in health and disease. Microglia, the primary innate immune cells in the CNS elicit a protective immune response during an acute brain injury. Microglia are primed with aging. Chronic activation of microglia by Aβ triggers the persistent release of proinflammatory mediators, which can eventually cause neuronal death leading to AD.

1.2.2. Oxidative stress

In health, low levels of ROS are fundamental to maintain normal physiological functioning, but increased ROS levels are associated with oxidative damage of various cellular compartments and molecules. Oxidative stress is a condition where ROS production exceeds the cellular antioxidant defense system. All organisms have developed adaptive responses to oxidative stress that result in an increased production of defensive enzymes, molecular chaperones and antioxidant molecules In the cell, the main protective system is represented by enzymatic and non-enzymatic antioxidant factors, such as superoxide dismutase (SOD), glutathione (GSH) peroxidase (GPX), vitamins, and carotenoids[102]. ROS can be generated through several pathways such as direct interactions between redox-active metals and oxygen species, reactions, or by indirect pathways

involving the activation of enzymes like nitric oxide synthase (NOS) or nicotinamide adenine dinucleotide phosphate (NADPH) oxidase[103]. It is known that age-related memory impairments correlate with a decrease in brain and plasma antioxidants defense mechanism[104].

In 1954, Denham Harman proposed that free radical reactions "may be involved in production of the aging changes associated with the environment, disease and an intrinsic aging process"[105]. Time has confirmed that free radicals are involved in the aging process, as well as diseases associated with aging, as AD[106]. The increased production of ROS during aging is most relevant to the CNS, which consumes 20% of the body's oxygen and, at the same time, is highly vulnerable to oxidative stress also because of the relative low presence of antioxidant enzymes[107]. The brain's susceptibility to oxidative stress leads to an increase in oxidative biomarkers, as toxic levels of metals, DNA damage, and impaired protein metabolism. The electron transport chain (ETC) is the enzymatic system responsible for cellular energy production, which also results in ROS production that makes mitochondrial DNA (mtDNA) particularly susceptible to oxidative damage[102]. This condition is responsible for the progressive impairment of mitochondria implicated both in aging and in AD. The interaction between oxidative stress and mitochondrial dysfunction likely forms a vicious spiral that amplifies the alterations observed in AD[108]. According to the mitochondrial cascade hypothesis, the mitochondrial dysfunction together with environmental factors are leading cause for AD, driving disease's features as Aβ production, tau phosphorylation, synaptic degeneration, and oxidative stress[109]. Indeed, oxidative stress can modulate pathways involved in AD pathogenesis, as p38, a member of the mitogen-activated protein kinases (MAPKs) family activated during Aβ-mediated oxidative stress. In a primary neuronal model, this kinase also showed to induce tau phosphorylation, which could be counteracted by pretreatment with an inhibitor of p38[110].

Advanced glycation end products (AGEs) are generated by a non-enzymatic reaction of sugars to proteins, that become potent neurotoxins and proinflammatory molecules[111]. During all life AGEs are accumulated, also in the brain, where they colocalize with tau and Aβ proteins generating irreversibly cross-linked heterogenous aggregates. Indeed, extracellular accumulation of AGEs. Free radicals are involved in this glycation processes and can enhance the formation of Aβ cross-linking[112]. Moreover, the activation of AGEs' receptor (RAGE) induces an inflammatory response which in turn upregulates the expression of the receptor, creating a vicious cycle[113].

We can affirm that aging, inflammation and oxidative stress represent an inseparable triad, in which all of them contribute equally and feed others creating a positive feedback loop. This scheme is summarized in the "error catastrophe theory" which proposes that damages to cell constituents accumulate during aging. At the same time, cellular defense mechanisms weaken, thus the accumulated damages cannot be repaired efficiently, leading to loss of function and finally cell death[111]. This condition contributes to the development of neurodegenerative diseases as AD and, at the same time, characterize the cellular environment of the pathology.

1.3. Endoplasmic Reticulum stress and the Unfolded Protein Response

The endoplasmic reticulum (ER) is the largest multifunctional organelle in the cell and the major site of protein synthesis, folding, and transport, lipid and steroid synthesis, carbohydrate metabolism and calcium storage[114,115]. The numerous functions of this organelle require a complex structure to coordinate all of them and to respond actively to changes in the intracellular environment. Thus, ER has numerous contact sites with all membrane-bound organelles, including the plasma membrane, mitochondria, Golgi, endosomes, and peroxisomes[116].

The ER consists of a nuclear envelope and a periphery represented by smooth tubules and rough sheets. ER is defined as an interconnected network with a continuous membrane, that shows different structures with specific functions in the cell. The nuclear envelope has an inner nuclear membrane (INM) and an outer nuclear membrane (ONM), and shares a common lumen with the peripheral ER. The nuclear envelope, which show numerous pores to allow the transport of RNAs and proteins, is connected to sheets of the peripheral ER. These rough sheets, as defined by the high density of ribosomes on the cytosolic surface, are the principal site of synthesis, folding and post-translational modifications for proteins. On the contrary tubules, that do not show many ribosomes, are dynamic, and continually rearranging and growing[117] (Fig. 7). The morphology and intracellular location of the ER subdomains contribute to the function of these structures and hence the role of the specialized cell in which they are located.

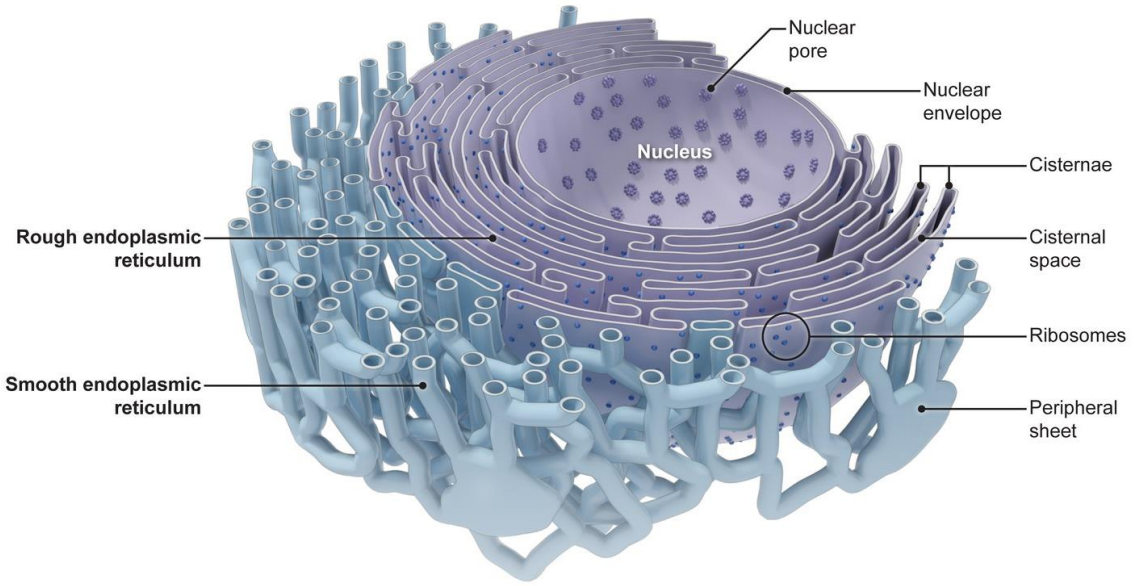

Figure 7. The endoplasmic reticulum (ER) consists of various interconnected shapes. At the center of the cell, the nuclear envelope contains pores that control what molecules enter and exit the nucleus. The nuclear envelope is also connected to the stacked sheets (cisternae) of the rough endoplasmic reticulum, which is specialized for protein production. From the rough endoplasmic reticulum, the tubules of the smooth endoplasmic reticulum (blue) form a network that extends across the cell and is interspersed with sheet-like structures (peripheral sheets).

The ER is the principal site for biosynthesis of proteins, post-translational modification, folding and assembly of newly synthesized proteins. If the protein is destined to be an integral membrane protein, it will be translocated and anchored to the phospholipid bilayer. The proteins destined to secretion, after the synthesis and translocation into the ER lumen, they must be properly folded and modified, with the aid of chaperones and folding enzymes. These modifications include N-linked glycosylation, disulfide bond formation and oligomerization[114]. At this point the fate of the proteins is determined, and it will be released by the chaperones and packaged for travel through the Golgi to the site of destination (such as the plasma membrane or secreted) or move into peroxisomes[115]. Under physiological conditions, chaperones resident in the cytosol and the ER ensure the correct folding of newly synthesized proteins, and quality control mechanisms identify misfolded proteins to enable their degradation via the proteasome, lysosome and autophagy pathways[118].

The ER is extremely sensitive to changes in its structure, integrity, and function. In some cases, even with several proteins and complexes dedicated to folding proteins properly, a fraction of proteins does not complete the functional form and are either misfolded or aggregated[119].

If the final tertiary structure cannot be achieved, unfolded proteins are translocated to the cytosol where they will be ubiquitinated and degraded by a proteasome-dependent

way, known as ER-associated degradation (ERAD) pathway to avoid that aberrant polypeptides enter the secretory pathway[120] (Fig. 8).

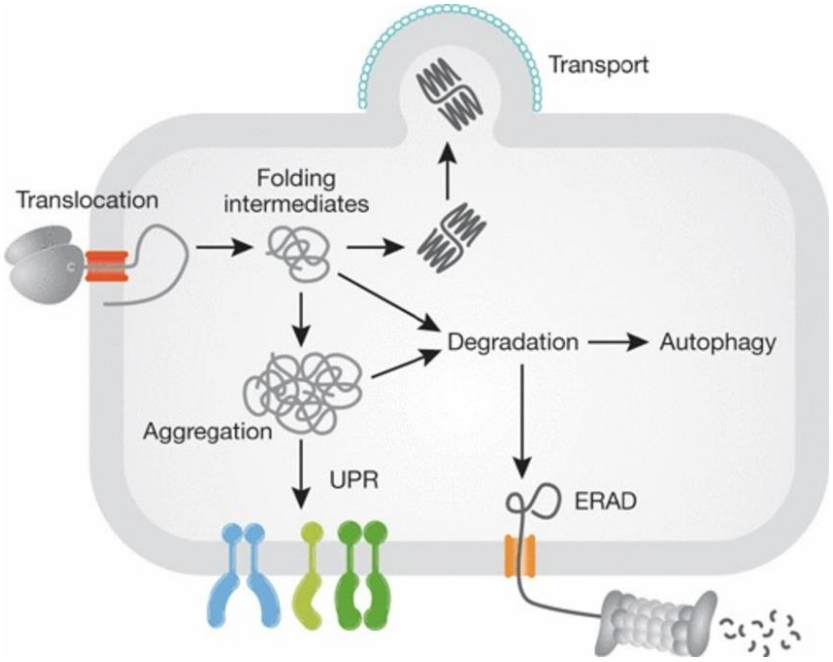

Figure 8. The general ERAD pathway for degradation of misfolded ER proteins. ERAD is initiated on the recognition of non-native proteins as aberrant molecules by quality control receptors. These terminally misfolded or unassembled proteins are then sorted to an ER-membrane-associated dislocation/ubiquitination complex containing adaptor proteins that recognize the quality control receptor and/or the ERAD substrate directly. A translocon then acts as a conduit for the retrotranslocation of the protein to the cytosol, and this process is often coupled with ubiquitination by an ER-associated E3 ubiquitin ligase. Cytosolic components are also recruited to the retrotranslocation complexes to aid in the extraction of the ERAD substrate from the ER, and prepare the substrate for proteasomal degradation.

Misfolding can occur due to the unique environment of the lumen and the high protein concentration of both newly synthesized proteins, proteins ready for secretion, and proteins that act as molecular chaperones and folding enzymes. Logistically, due to the high protein concentration and packing in the lumen, the folding enzymes must first identify and find the proper target protein to initiate the folding process. In presence of misfolded proteins, there are several things that must occur to hold balance and proper function, including translational inhibition, degradation of aberrant proteins, and an increase in the production of chaperones and folding enzymes to restore normal activity of the ER and the cell. If the balance is not restored, the failure of the ER to reduce the excessive protein load leads to “ER stress” and eventually to cell death or apoptosis[121].

These cellular responses are the results of an integrated intracellular signaling cascade known as the unfolded protein response (UPR)[122]. The UPR can be viewed as a simple signal transduction pathway that involves two main actors: stress sensors at the ER membrane, and downstream transcription factors that modulate gene expression to reduce stress or to induce pro-apoptotic responses[123]. The UPR target genes vary

depending on the tissue context and the type of physiological perturbation that causes ER stress. The first action of the UPR is to enlarge ER to satisfy the needs of the cell to properly fold the proteins, through the generation of sheets and to increase the ER folding machinery[124]. The UPR is controlled by three sensor transmembrane proteins activated upon stress: inositol-requiring enzyme 1α (IRE1α), protein kinase RNA-like ER kinase (PERK), and activating transcription factor 6 (ATF-6)[122](Fig. 9).

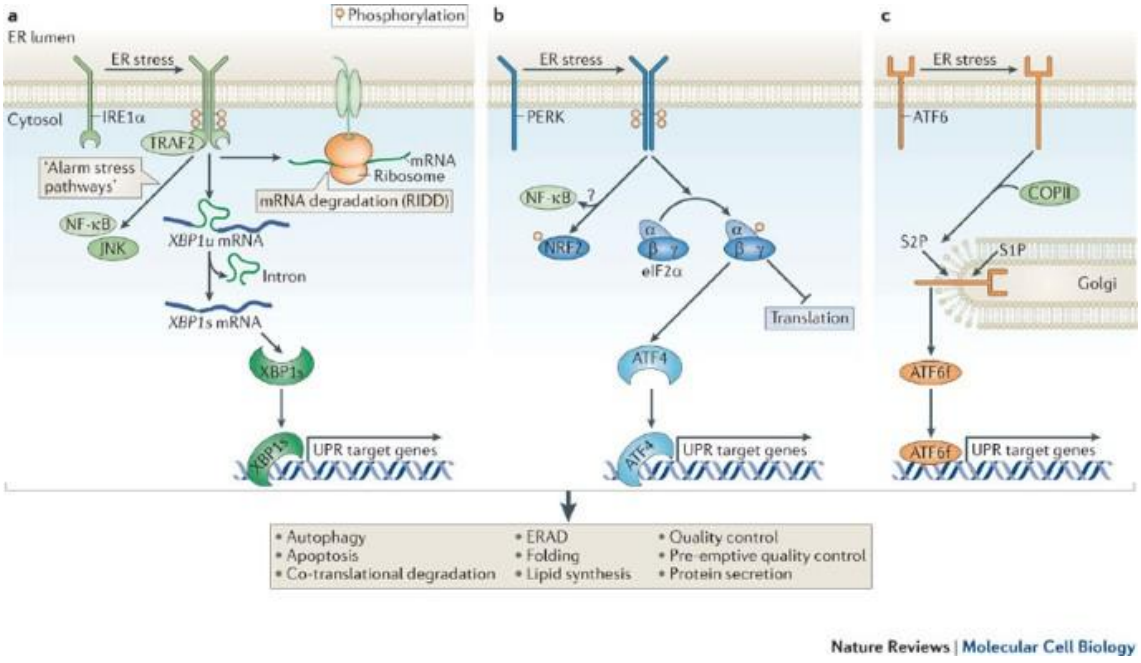

Figure 9. The unfolded protein response (UPR) stress sensors, inositol-requiring protein 1α (IRE1α), protein kinase RNA-like endoplasmic reticulum (ER) kinase (PERK) and activating transcription factor 6 (ATF-6), transduce information about the folding status of the ER to the cytosol and nucleus to restore protein-folding capacity. a: IRE1α dimerization, followed by autotransphosphorylation, triggers its RNase activity, which processes the mRNA encoding unspliced X box-binding protein 1 (XBP1u) to produce an active transcription factor, spliced XBP1 (XBP1s). XBP1s controls the transcription of genes encoding proteins involved in protein folding, ERAD, protein quality control and phospholipid synthesis. IRE1α also degrades certain mRNAs through regulated IRE1-dependent decay (RIDD) and induces 'alarm stress pathways', including those driven by JUN N-terminal kinase (JNK) and nuclear factor-κB (NF-κB), through binding to adaptor proteins. b: Upon activation, PERK phosphorylates the initiation factor eukaryotic translation initiator factor 2α (eIF2α) to attenuate general protein synthesis, and it may also phosphorylate nuclear factor erythroid 2-related factor 2 (NRF2), a transcription factor involved in redox metabolism. Phosphorylation of eIF2α allows the translation of ATF-4 mRNA, which encodes a transcription factor controlling the transcription of genes involved in autophagy, apoptosis, amino acid metabolism and antioxidant responses. c: ATF-6 is localized at the ER in unstressed cells. In cells undergoing ER stress, ATF-6 is transported to the Golgi apparatus, where it is processed by site 1 protease (S1P) and S2P, releasing its cytosolic domain fragment (ATF6f). ATF6f controls the upregulation of genes encoding ERAD components and also XBP1. At the bottom of the figure, general UPR outcomes, which may or may not require transcription, are presented.

In physiological conditions these proteins are inactivated by the binding to the chaperone 78KDa glucose-regulated protein (GRP78), also known as BiP. In ER stress, BiP is released to induce the dimerization and autophosphorylation of PERK and IRE1α, as well as the proteolysis of ATF-6, leading to the production of transcription factors that activate UPR genes[122].

Upon activation, IRE1α leads to the splicing of XBP1, which results in the expression of an active and stable transcription factor called XBP1s. The activity of XBP1s can be defined as pro-survival because support proteostasis by inducing the expression of genes involved in protein folding and quality-control mechanisms, and by activating the ERAD[125]. In addition, IRE1α targets a group of mRNAs and microRNAs for degradation through a process known as regulated IRE1α-dependent decay (RIDD) which has pleiotropic effects in cells, as it is able to modulate the expression of different proteins leading to stress mitigation, inflammation and apoptosis[126]. Under prolonged stress, IRE1α activates autophagy, inflammatory pathways that involve nuclear factor-κB (NF-κB), and the apoptotic-signaling kinase-1 (ASK1), followed by the activation of downstream kinases, Jun-N-terminal kinase (JNK) and p38 mitogen-activated protein kinase (p38 MAPK), leading to apoptosis[125,127]. Furthermore, IRE1 RNase activity promote the degradation of ER-associated RNAs to reduce the translational load on the ER by removing mRNAs that otherwise would be translated[128]. Thus, IRE1α has a dual role in the response to chronic ER stress, mediating adaptation through XBP1s and mediating induction of apoptosis via the MAP kinase pathway and RIDD.

ER stress triggers also the activation of PERK which is directly responsible for the phosphorylation of the α subunit of eukaryotic translation initiation factor (eIF2α). Phosphorylated eIF2α (p-eIF2α) inhibits protein synthesis and consequently prevents an overload of proteins in the ER lumen[122]. Furthermore, p-eIF2α promotes the selective translation of ATF-4 which upregulates genes related to apoptosis, including the pro-apoptotic factor CHOP, ROS and members of the apoptosis regulator BCL-2 family [125,129].

Finally, ATF-6 is the third mediator of UPR that, in ER stress, translocates from the ER to the Golgi apparatus, where it is cleaved by endopeptidase S1P and endopeptidase S2P to release a fragment called ATF-6f that includes the transcription factor domain. Once activated, ATF-6 is transferred into the nucleus where it promotes the transcription of several genes that encode proteins involved in redox control, amino acid metabolism, autophagy, protein folding and synthesis[130].

Although it is clear that ER-stress leads to large scale changes in the protein and RNA content of the ER, it is not yet clear if this determines a direct structural reorganization in order to satisfy the new needs of the organelle. Overall, UPR mediators are involved in maintaining ER homeostasis. Excessive or long-term accumulation of

misfolded proteins leads to the failure of UPR's adaptive responses and the initiation of the regulated cell death.

1.3.1. Endoplasmic Reticulum stress and the Unfolded Protein Response in Alzheimer's disease

Numerous neurodegenerative diseases, as AD, are characterized by the progressive loss of neuronal function in defined regions of the CNS, culminating in severe dysfunction. These conditions have distinct pathophysiological and clinical hallmarks, but the abnormal aggregation of misfolded proteins is a common feature of all of them, indeed they are often described as protein misfolding disorders (PMDs)[131]. Importantly, impairment of proteostasis is also exacerbated during ageing, the main risk factor for PMDs[132]. Neuronal cells are particularly sensitive to protein misfolding that leads to disrupted function of synapses, apoptosis and selective neuronal death[133]. Furthermore, misfolded proteins lose their physiological activity and acquire neurotoxicity leading to chronic inflammation[131]. One consequence of accumulating misfolded protein is the generation of ER stress that play a pivotal role in the pathophysiology of PMDs[134]. Interestingly, in patients' brains affected with PMDs, ER stress markers often co-localize with protein aggregates[135]. For example, in AD, many studies have indicated that Aβ oligomers, which can accumulate in the ER lumen, cause disruption of ER calcium homeostasis, resulting in a proapoptotic ER stress response[136].

The mechanisms leading to AD are complex and related to changes in synaptic transmission, altered calcium homeostasis, increased ER stress and a chronic state of neuroinflammation[137]. During AD, the continuous accumulation of Aβ or p-tau results in a drastic alteration of ER calcium homeostasis, abnormal protein folding and ER stress. Tau has been shown to block the ERAD pathway leading to the accumulation of misfolded proteins in the ER lumen, while Aβ oligomers induces the disruption of the cytosolic calcium balance, provoking ER stress-dependent cell death, synaptic depression and spine elimination[138]. In brain tissue of AD's patients, it is possible to observed increased levels of UPR activation markers as compared to control brain tissue from healthy individuals. Indeed, high expression levels of the chaperone BiP, PERK and IRE1α have been observed in AD neurons that contain abnormally phosphorylated tau[139]. Remarkably, levels of IRE1α phosphorylation directly correlated with the Braak stage of pathology in patients with AD[140].

The UPR can show opposite effects depending on the disease stage, first as a pro-survival factor to sustain proteostasis, but then shifting promoting cell damage in the symptomatic phases. ER stress is not only a consequence of deleterious effects on the secretory pathway, but also can trigger a vicious cycle by increasing aggregation of disease-associated proteins. First, under mild ER stress, UPR has a proadaptive response to alleviate the ER protein overload and preserve neuronal viability. The activation of the UPR can counterbalance protein aggregation by improving protein folding and promoting clearance pathways, such as ERAD and autophagy. However, in long-termed ER stress, the ER stress-mediated cell death program will lead to neuronal loss and neurodegeneration. Some researchers have suggested that ER stress may play only a minor role in the mechanisms of neurodegeneration[141]. ER stress in chronic neurodegenerative disorders often stimulates autophagic activities, however, failure in clearing the aggregated proteins and the impairment of UPR or autophagy lead to the accumulation of misfolded proteins and the progression of neurodegeneration[142]. Autophagy is an important mechanism, especially for neurons that are unable to dispose misfolded proteins[143]. ER stress may regulate autophagy via the PERK/eIF2α/ATF-4 signaling pathway. The accumulation of tau protein triggers the phosphorylation of PERK and eIF2α that are markedly increased in AD brains, especially in the hippocampal pyramidal cells and the frontal cortex[144].

The activation of PERK was shown to be associated with increased expression of the transcription factor ATF-4 and BACE1 indeed, in a mouse model of AD, its insufficiency was associated with a lower BACE1 expression and reduced levels of Aβ peptides[145]. Indeed, the presence of Aβ oligomers in the hippocampus was associated with increased ATF-4 which, in response to ER stress, induces the transcription of autophagy genes and the inhibition of eIF2α dephosphorylation accelerating human cell death in the axonal compartment[146]. Beyond its role as a mediator of ER stress in all cells, chronic PERK signaling modulates neuronal plasticity and behavior, regulating the expression of a cluster of synaptic proteins relevant in neurodegenerative disease. It has been demonstrated that, in a mouse model of AD, chronic PERK signaling has adverse effects on synaptic function, and its deletion improved memory deficits and long-term potentiation[147]. Indeed, PERK may directly phosphorylate and activate GSK3β, leading to the hyper-phosphorylation of tau, increased Aβ generation and deficits in learning and memory accompanied with neurodegeneration[148].

Furthermore, a positive correlation between the progression of AD histopathology and the activation of IRE1 was detected in human brain tissue. Genetic ablation of the RNAse domain of IRE1 in the CNS significantly reduced Aβ deposition and restored synaptic and cognitive function. It is worth noting that IRE1 deficiency restored the learning and memory capacity of AD mouse model[140]. The role of IRE1α signaling on neurodegeneration has been studied extensively in the context of downstream XBP1 function, and most studies suggest that XBP1s has a neuroprotective role by control the stability of APP protein, which accelerated the amyloid cascade. Moreover, a polymorphism in the promoter of the transcription factor XBP1 was identified as a risk factor for AD[149]. Furthermore, XBP1 can reduce the expression of BACE1, through HRD1, leading to the reduction in Aβ plaques and can upregulate the expression of catalytic components of the ERAD machinery[150].

Few evidences about the role of ATF-6 in AD has been reported but Du et al. have shown that ATF-6 can reduce the expression of APP to suppress the Aβ level, downregulate the promoter activity and expression of BACE1, and protect the retention of spatial memory in AD model mice[151].

Finally, as a consequence of prolonged ER stress, an increase of pro-apoptotic UPR components has been found in AD brains, likely causing neurodegeneration. Amon them, the main transcription factor linking ER stress to apoptosis, CHOP, was found upregulated in the brains of AD patients[152]. ER stress-mediated CHOP activation plays a central role in the triggering of AD pathological hallmarks, increasing ROS formation, oxidative stress, inflammation, and apoptotic neuronal death[153].

2. AIM

Neurodegenerative diseases are frequently an age-related condition and, with the consistent increase in life expectancy, in the last 20 years the number of diagnoses is prominently enhanced, becoming a central problem not only for patients but also for the entire health system[2]. Unfortunately, despite the effort spent from all over the scientific world; to date only symptomatic treatments, able to reduce symptoms but not to counteract the progression of the disease, or to restore the correct neuronal function, are available. One crucial reason is represented by the fact that the diagnosis usually occurs late in the evolution of these pathology, when cellular death involves a great number of neurons.

Although their etiopathology is yet to be clarified, chronic neurodegenerative diseases have a multifactorial nature. In this regard, several studies in the biochemical, pharmacological and toxicological fields have highlighted the involvement of multiple cellular and molecular factors, such as increased oxidative stress, mitochondrial dysfunction, and inflammation[154]. Despite the fact that neurodegenerative diseases have distinct pathophysiological and clinical hallmarks, the abnormal aggregation of misfolded proteins is a common feature for all of them. Moreover, the failure of the proteostasis system is also aggravated during ageing, the main risk factor for these conditions[132]. Neurons are particularly sensitive to protein misfolding responsible for synapses' failure, apoptosis, and chronic inflammation[133].

AD is the most frequent neurodegenerative disease and represents the leading cause of dementia worldwide in the elderly[8]. One crucial reason is represented by the fact that the diagnosis usually occurs late, when cellular death involves a great number of neurons. In this view, new biomolecular markers to provide an early diagnosis, could represent a critical step in the research for innovative therapeutic approach in the treatment of AD.

Furthermore, disease-modifying therapy has to be started years before of potentially irreversible pathologic changes have occurred to prevent cognitive impairment and extensive neuronal loss.

The aim of the presents work was to identify potential new biomarkers significantly dysregulated in AD, with particular attention to ER stress that characterize not only neurodegeneration but also the aging process. For this purpose, in this project it has been used an integrated approach of behavioral test, bioinformatics and biomolecular analysis in a murine model of AD induced by intracerebroventricular injection of $A\beta_{1-42}$ oligomers at different ages.

Considering the pivotal role of aging in the neurodegenerative process, the treatment and all the analysis have been conducted on young, 3 months old mice, and old, 18 months old mice. The cognitive deficit due to AD and age have been assessed with behavioral test, such as Y-maze and Morris water maze. After the behavioral investigation the mice have been sacrificed. The following tests were carried out on the hippocampal section of young and aged mice, both healthy and with AD. RNA was extracted to perform an RNA sequencing analysis that allowed us to identify, through bioinformatics software as Gene Set Enrichment Analysis (GSEA), Protein ANalysis THrough Evolutionary Relationships (PANTHER), and Gene Ontology enRIchement anaLysis and visuaLisAtion (GOrilla), several pathways and molecular functions involved in the cellular response to AD and aging and different dysregulated genes. The main biological pathway seems correlated to stress and apoptotic cellular death, while among the genes one of particular attention was Mapkapk5. Finally, these functions and the UPR were investigated by Western Blotting to confirm our data.

3. METHODS

3.1. Reagents

$A\beta_{1–42}$ peptides were purchased by AnaSpec (Fremont, CA, USA). Aprotinin, bovine serum albumin (BSA), CHAPS, 2'7'-dichlorodihydrofluorescein diacetate (DCFH-DA), dimethyl sulfoxide, 5,5′-dithiobis (2-nitrobenzoic acid), dithiothreitol, EDTA, ethanol, glycerol, Hepes pH 7.4, hexafluoroisopropanol, leupeptin, β-mercaptoethanol, sodium chloride, sodium fluoride, sodium orthovanadate, sucrose, sulfosalicylic acid, Triton-X 100, tris pH 7.5, and primary antibody anti-β-actin was provided by Sigma-Aldrich (St Louis, MO, USA). Paraformaldehyde solution (4%) was provided by Santa Cruz Biotechnology (Dallas, TX, USA) and NP-40 was from Roche Diagnostic (Risch, Switzerland). Primary antibodies phospho-GSK3α/β (Ser21/9) and GSK3α/β, phospho-p44/42 MAPK (ERK1/2, Thr202/Tyr204), phospho-Akt and Akt, ATF-6, phosho-eIF2α and eIF2α, IRE1α, PERK, p44/42 MAPK, were provided by Cell Signaling Technologies Inc. (Danvers, MA, USA). Mapkapk5 antibody was purchased from EpigenTek (Farmingdale, NY, USA). Secondary anti-mouse and anti-rabbit antibodies were purchased from Jackson ImmunoResearch Europe Ltd (Ely, Cambridgeshire, UK). Bradford assay solution, Laemmli sample buffer, enhanced chemiluminescence (ECL) solution, Tris buffered saline (TBS), and Tween 20 were purchased from Bio-Rad Laboratories S.r.L. (Hercules, CA, USA). RNeasy® Plus Mini Kit and Qiaseq Stranded total RNA library were purchased from Qiagen S.r.L. (Milan, Italy). Agilent RNA 6000 nano assay and High sensitivity DNA assay were provided by Agilent Technologies Italia S.p.A. (Cernusco sul Naviglio (MI), Italy). Illumina Neoprep stranded RNA-seq library preparation kit was provided by Illumina Inc (San Diego, CA, USA). The Qubit 1x ds DNA HS kit was purchased from Thermo Fisher Scientific

(Waltham, MA, USA) All experiment reagents were reagent grade and commercially available.

3.2. Animals

Adult male C57Bl/6 mice (10 weeks old, 25–30 g body weight; Charles River Laboratories Italia Srl, Calco (LC), Italy) were utilized. The mice were housed in a temperature-controlled room (23–24°C) with free access to food and water and presented with 12 h light/12 h dark cycles. Experimental procedures were carried out in the light cycle (from 9:00 a.m. to 3:00 p.m.) including control groups in any tests utilized. Briefly, procedures on the mice were carried out according to the European Communities Council Directive 2010/63/EU and the current Italian Law on the welfare of the laboratory animal (D.Lgs. n.26/2014). The animal protocol was approved by the Italian Ministry of Health (Authorization No. 291/2017-PR) and by the corresponding committee at the University of Bologna. The number of experimental animals was minimized, and care was taken to limit mice suffering. Mice were allowed to acclimatize for at least 2 weeks before the start of experiments.

3.2.1. Experimental design

The animals were randomized into four groups (n = 7/group): 3Vh, 3Aβ, 18Vh, and 18Aβ. Two groups were treated, one at 3 and one at 18 months, with $A\beta_{1\text{-}42}$ oligomers by a unilateral intracerebroventricular (i.c.v.) injection, while the others received, at the same age of the lesioned animals, a unilateral i.c.v. injection of saline solution (sham groups). After 10 days from the lesion induced, the mice underwent behavioral assessment. After the behavioral analysis, the animals were deeply anesthetized before being sacrificed by cervical dislocation to collect the samples for biomolecular analysis.

3.2.2. $A\beta_{1\text{-}42}$ oligomers preparation and injection

$A\beta_{1–42}$ peptides (AnaSpec) were solubilized to 1 mg/ml in hexafluoroisopropanol before being sonicated and lyophilized at room temperature. The unaggregated $A\beta_{1–42}$ film obtained was dissolved to a final concentration of 1 mM with sterile dimethylsulfoxide and stored at −20°C until use. Briefly, to enhance oligomer formation, the $A\beta_{1\text{-}42}$ stock was diluted in saline buffer at 40 μM and incubated for 48 h at 4°C[155,156].

Animals were anesthetized under gaseous anesthesia (2% isoflurane in 1 L/min O_2/N_2O) using a gaseous anesthesia system (Ugo Basile, Varese, Italy) and then mice were positioned on a mouse stereotaxic frame (myNeuroLab, Leica-Microsystems Co, St. Louis, MO, USA). Anesthesia was maintained with 1.5% isofluorano/O_2 (1L/min). The scalp was incised to reveal the skull and recognize the bregma to set coordinates. Six microliters of $A\beta_{1-42}$ oligomers (40 μM) were injected i.c.v. using a 10-μL Hamilton syringe, at a rate of 0.5 ml/min. After the injection, the needle was left in place for a few minutes before being retracted slowly and the wound was cleaned and sutured (Histoacryl, Aesculap AG, Germany). The sham mice received the corresponding volume of saline. The following coordinates were used: anteroposterior: +0.22, mediolateral: +1.0, dorsoventral: −2.5, with a flat skull position. After the surgery mice were collocated under an irradiating lamp to promote the recovery for the time required.

3.3. Behavioral analysis

All the tests were performed between 9.30 a.m. and 3.30 p.m. All scores were attributed by a blinded observer.

3.3.1. Y-maze test

The spatial working memory was evaluated by recording spontaneous alternation behavior in the Y-maze as described earlier[157]. Briefly, each arm of the maze (Ugo Basile® S.r.L., Gemonio (VA), Italy) was 35 cm long, 15 cm high, and 5 cm wide and converged to a 120° angle. The mice were positioned at the end of the A arm and allowed to move freely through the maze for 5 min. The entry in all three arms consecutively was counted as an alternation. Thus, the number of maximum alternations was calculated as the total number of arm entries minus two and the percentage of alternation was calculated as (actual alternations / maximum alternations) × 100[158].

3.3.2. Morris water maze test

The test was performed using a circular plastic tank (1.0 m diameter, 50 cm height) filled with water and milk (22°C). The maze was located in a room containing several simple visual, extra-maze cues that were constant throughout the study. A transparent platform was set inside the tank and its top was submerged 1.5 cm below the water surface in the center of one of the four quadrants of the maze[159].

A camera was placed to register mice's movements and send data to an automated tracking system (EthoVision, Noldus, The Netherlands). For each training trial, animals were placed into the pool at one of the four positions selected randomly, and the latency to find the hidden platform was recorded. The platform was located in a constant position throughout the test period in the middle of one quadrant. Mice that could not reach the platform within 60 s were guided to it by the experimenter and allowed to remain there for 10 s. After the trial, each mouse was placed under a warming lamp in a holding cage for 25 s until the next trial. Training trials were conducted four times a day for 5 days. On day 6, the platform was removed, and animals were allowed to swim freely for 60 s. During the probe trial the escape latency and the frequency in the platform zone were recorded.

3.4. Tissue preparation for neurochemical analysis

At the end of behavioral tests, the mice were deeply anesthetized and sacrificed by cervical dislocation. The brains were quickly removed, and the hippocampi of each hemisphere were isolated on ice and transferred to liquid nitrogen. For the protein extraction, the tissues were homogenized in lysis buffer (50 mM Tris, pH 7.5, 0.4% NP-40, 10% glycerol, 150 mM NaCl, 10 μg/ml aprotinin, 20 μg/ml leupeptin, 10 mM EDTA, 1 mM sodium orthovanadate, 100 mM sodium fluoride) and the cytoplasmic protein concentration was determined by the Bradford method[160].

Total RNA was isolated from hippocampus using RNeasy Plus mini kit (Qiagen). Briefly, the samples were lysed on ice with 1% β-mercaptoethanol by using a homogenizer SHM1 (Stuart, Bibby Scientific LTD, Staffordshire, UK). The samples were then added to an equal volume of 70% ethanol. The solution was filtered using a cartridge containing a clear silica-based membrane to which the RNA binds. RNA was finally eluted with RNase-free water and stored at −80°C.

RNA integrity was evaluated with Agilent RNA 6000 nano kit using Agilent 2100 Bioanalyzer System (Agilent) by spectrophotometric analysis. Libraries were then prepared using Qiaseq Stranded total RNA library (Qiagen) and their quantification was assessed with the High sensitivity DNA assay (Agilent) using Agilent 2100 Bioanalyzer System (Agilent), and again with the Qubit 1x ds DNA HS kit using Qubit (Thermo Fisher Scientific). Finally, two pools were prepared with each sample at the concentration of 2,000 pM for the library sequencing.

3.4.1. RNA-seq analysis

RNA sequencing was carried out according to the Illumina pipeline on a NextSeq 500 Instrument (Illumina, San Diego, CA, USA) using the NextSeq High Output kit v2 (150 cycles) (Illumina). Obtained sequences were mapped to the mouse genome (GRCm38) using the algorithm HISAT2[161] and a pre-built genome index downloadable from HISAT2 website. Then, StringTie[162] was used to assemble and quantify the transcripts in each sample. Finally, expressed transcripts have been normalized using the DeSeq2 package for R. Differential gene expression and downstream analyses were performed using DEseq2 and custom R scripts[163]. For the analysis, gene differential expression test between 3Vh, 3Aβ, 18Vh and 18Aβ groups were performed for different age and treated and not treated mice (3 months treated/not treated, and 18 months treated/not treated) by their log2 fold change (log2FC) from the basal-state. As cutoff criteria we used at least in one comparison p-value of < 0.05 and $-2 < \log2(FC) > 2$.

3.4.2. Bioinformatic analysis

Gene expression analysis was performed using Broad gene set enrichment analysis GSEA tool[164] and TOPPGENE tool[165].The C2 curated genes was used as background gene sets using the MsigDB database (http://software.broadinstitute.org/gsea/msigdb/, version 7.4). The screening of upregulated and downregulated gene sets for each analysis (3Vh vs. 18Aβ, 3Aβ vs. 18Aβ, and 18Vh vs. 18Aβ) were performed using GSEA enrichment analysis, specific parameters were as follows: numbers of permutations (1000), collapsed datasets due to gene symbols (true), enrichment statistic (classic), metrics for gene ranking (Signal2Noise), gene list sorting model (real), gene list ordering mode (descending), max size (500), and min size (15). The Gene ontology (GO) terms were evaluated with broad tool GOrilla[166] and PANTHER Classification system[167].

3.4.3. Determination of cellular redox status

The redox status, in terms of ROS formation, was evaluated by measuring the oxidation of DCFH-DA to 2′7′-dichlorofluorescein (DCF)[168]. The samples (60 µl) were incubated for 30 min with 2 mg/ml of DCFH-DA, to allow the DCFH-DA to be incorporated into any membrane-bound vesicles and the diacetate group to be cleaved by esterases. At the term of incubation, the conversion into the fluorescent product DCF was measured (excitation at 485 nm, emission at 535 nm) using a microplate reader (GENios,

TECAN®). Background fluorescence (conversion of DCFH-DA in the absence of homogenate) was corrected by the inclusion of parallel blanks. The values were normalized to protein content and expressed as the mean ± SEM of fluorescence intensity arbitrary units (UF) of each experimental group.

3.4.4. Determination of glutathione content

Glutathione (GSH) content was assessed on samples (50 µL) precipitated with 100 µL of sulfosalicylic acid (4%). The samples were kept at 4°C for at least 1h and then subjected to centrifugation at 3000 rpm for 10 min at 4°C. A volume of 25 µl of the assay mixture and 50 µL of 5-5'-dithio-bis (2-nitrobenzoic acid) (4 mg/mL in phosphate buffer, 0.1 M, pH 7.4) was made up to a total volume of 500 µL. The yellow color that developed was read immediately at 412 nm (GENios, TECAN®) and the results were calculated using a standard calibration curve. The values were normalized to protein content and expressed as the mean ±SEM of GSH mmol/mg protein of each experimental group.

3.4.5. Western Blotting

The samples (30 µg proteins) were added to the Laemmli Sample Buffer 4x ((Bio-Rad Laboratories S.r.L.) and then separated on 4-15% TGX polyacrylamide gels (Bio-Rad Laboratories S.r.L.) in Running Buffer (25 mM Tris; 192 mM Glycine; 0,1% (w/v) SDS pH 8,3) for 30 minutes at 200 V. Before being electroblotted onto 0.45 µm nitrocellulose membranes in Blotting Buffer (25 mM Tris; 192 mM Glycine; 20% (v/v) MeOH pH 8,3) for 1 hour at 100 V, gels were photoactivated allowing the immediate visualization of proteins. After the transfer, the total protein signal was visualized by UV excitation to obtain normalization data for the next analysis, and membranes were incubated for 2 hours in Block Solution (5% no-fat powder milk; TBS; 0.05% Tween 20) to block aspecific binding sites. The membranes were incubated at 4°C overnight with primary antibody recognizing phospho-GSK3α/β (Ser21/9), phospho-p44/42 MAPK (ERK1/2, Thr202/Tyr204), phospho-eIF2α, PERK, ATF-6, phospho-Akt, IRE1α (1:1,000; Cell Signaling Technology Inc), or Mapkapk5 (1:1,000; EpigenTek). The next day, after washing with TBS-T (TBS + 0.05% Tween20), the membranes were incubated with a horseradish peroxidase (POD) linked anti-rabbit or anti-mouse secondary antibody (1:5,000; Jackson ImmunoResearch) for 1 hour at room temperature (RT). Immunoreactive bands were visualized by enhanced chemiluminescence (ECL; Bio-Rad

Laboratories S.r.L.). The same membranes were stripped (100 mM β-mercaptoethanol; 2% SDS; 62,5 mM Tris pH 6.7) and reprobed with GSK3α/β, p44-42 MAPK, Akt, eIF2α (1:1,000; Cell Signaling Technology Inc.), or anti-β-actin (1:1,000; Sigma-Aldrich) at 4°C overnight. The data were analyzed by densitometry, using Quantity One software (Bio-Rad Laboratories® S.r.L.). The values were normalized and expressed as the mean ± SEM of the densitometry in each experimental group.

3.5. Statistical Analysis

The data were analyzed with the PRISM 9 software (GraphPad Software, La Jolla, CA, USA) and expressed as mean ± SEM of each experimental group. The difference between the groups was analyzed by mixed model or one-way ANOVA with Tukey's post hoc test. The results were considered statistically significant when a p value was less than 0.05.

4. RESULTS

The effects of $A\beta_{1-42}$ oligomers in the UPR of young and aged mice was evaluated in a murine model of AD by i.c.v. injection of 6 μL of $A\beta_{1-42}$ oligomers in C57BL/6 mice at 3 and 18 months. Animals were divided into four experimental groups: two groups received i.c.v. injection of $A\beta_{1-42}$ oligomers at 3 or 18 months (3Aβ and 18Aβ), and two received the same amount of vehicle solution with the same modalities of others (3Vh and 18Vh).

Firstly, the cognitive impairment was evaluated in aged and lesioned mice through behavioral investigation. In particular, two cognitive tests were selected and performed starting from ten days after the lesion induced. The Y-maze test (Fig. 10A) and the Morris water maze test (Fig. 10B-D) were assessed to evaluate the spatial memory and learning impairment during the aging process and as a consequence for the $A\beta_{1-42}$ oligomers injection.

The Y-maze test showed in the aged groups (both healthy or lesioned) a significant reduction of the alternation percentage as compare to young animals (Fig. 10A). In the Morris water maze training, aged mice learned slowly the platform location as showed at day 2, but at the end of the training Aβ mice, both young or aged, spent more time to find the platform (Fig. 10B). During the probe trial the platform was removed and animals were allowed to swim freely in the pool. The latency for the first entry and the frequency in the platform zone were recorded (Fig. 10C-D). Results obtained showed an increase in the latency for the first entry and a decrease in the frequency in the platform zone in 3Aβ and 18Aβ mice, but significantly only in 18Aβ mice.

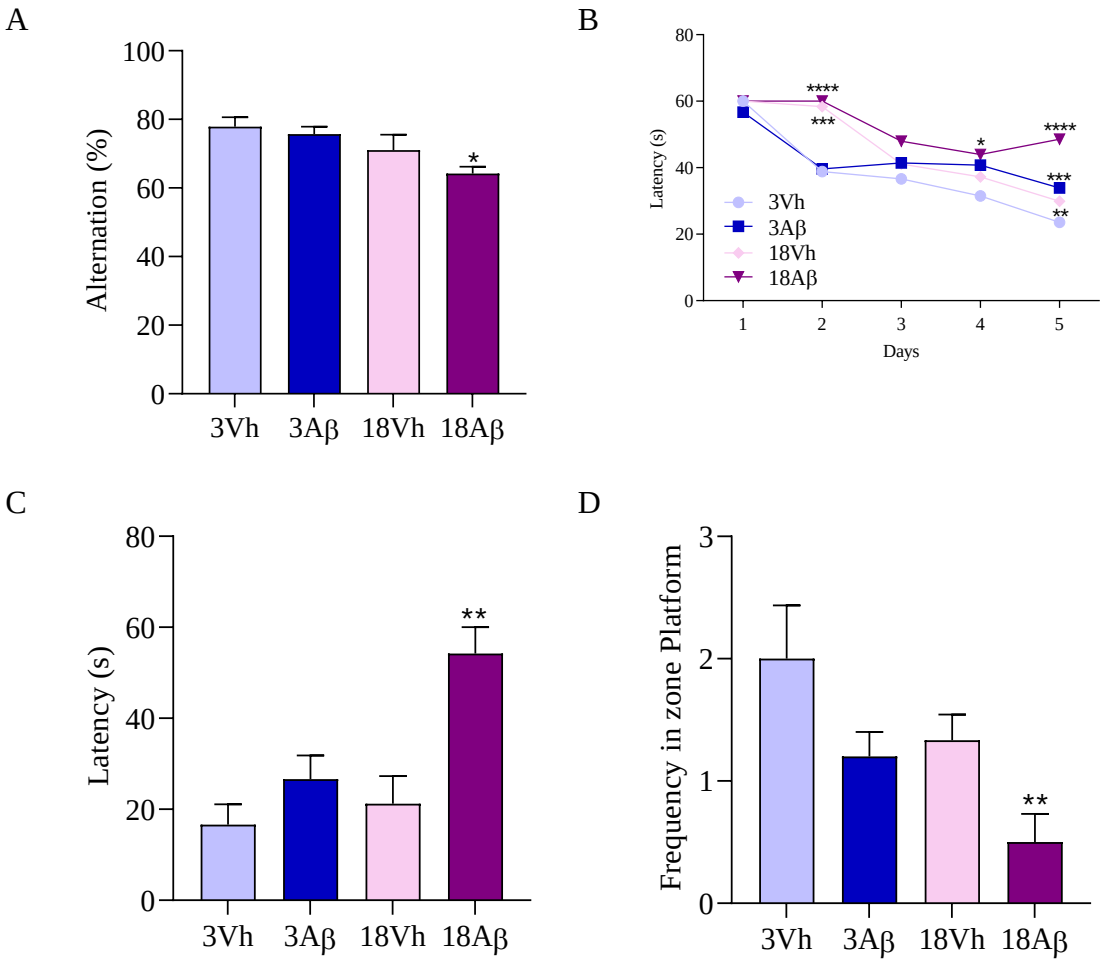

Figure 10. Effects of i.c.v. injection with $A\beta_{1-42}$ oligomers in young and aged mice on the performance in Y-maze test (A) and in the training (B) and probe trials (C-D) of the Morris water maze test (B-D). In the Y maze test the spontaneous alternation percentage was recorded in a 5 minutes trial. The training trials for the Morris water maze test were carried out for 5 days (four per day); the probe trial was performed on day 6- the escape latency (C), and the frequency in the platform zone (D) were recorded in the probe test. The values are expressed as mean ± SEM (n = 7) (A: *p < 0.05 vs. 3Vh and 3Aβ groups; B: day 2 ***p < 0.001 18Vh vs 3Vh and 3Aβ, ****p < 0.0001 18Aβ vs. 3Vh and 3Aβ; day 4 *p < 0.05 18Aβ vs. 3Vh; day 5 ****p < 0.0001 18Aβ vs. 3Vh, **p < 0.01 18Aβ vs. 3Aβ, **p < 0.01 18Vh vs. 18Aβ; C: **p < 0.01 vs. 3Vh, 3Aβ, and 18Vh; D: **p < 0.01 vs. 3Vh; mixed model or ordinary one-way ANOVA, post hoc test Tukey).

At the end of the behavioral assessment mice were sacrificed and the hippocampi of both hemispheres were extracted and proceeded for neurochemical analysis. Fifteen samples (4 samples for 3Vh, 3Aβ and 18Aβ, and 3 samples for 18Vh) were selected for RNA extraction and sequencing. RNA was extracted and purified with RNeasy® Plus Mini Kit (Qiagen) and then its integrity was evaluated with the Agilent RNA 6000 nano kit at the Agilent 2100 Bioanalyzer System (Agilent). Results obtained are shown in Table I and indicate a good quality sample, as evidenced by the RNA integrity value (RIN > 7).

Libraries were then prepared using the "QIAseq Stranded Total RNA Library Kit" and their quantification was assessed by bioanalyzer high sensitivity DNA assay and

Qubit, to obtain two pools with each sample at the concentration of 2,000 pM for the sequencing.

Table I. Summary of the RNA's integrity values (RIN) of selected samples

Sample 3 months	RIN	Sample 18 months	RIN
GGC0 Vh	7.70	GDC3 Vh	8.10
GGC3 Vh	7.40	GDC2 Vh	7.50
GAC2 Vh	7.60	GDC1 Vh	7.90
GBC4 Vh	7.50	GBC1 Aβ	8.00
GDC1 Aβ	7.80	GBC3 Aβ	7.80
GDC2 Aβ	8.10	GBC4 Aβ	7.70
GDC0 Aβ	8.10	GBC2 Aβ	8.00
GCC3 Aβ	7.60		

RNA sequencing was carried out and obtained sequences were mapped to the mouse genome (GRCm38). Finally, expressed transcripts have been normalized and differential gene expression and downstream analyses were performed using DEseq2 and custom R scripts[163]. To better understand the role of the aging process in our AD model and how it correlates with $A\beta_{1-42}$ oligomers neurotoxic activity, we performed the following investigation using three different sets of analysis. In the specific, we compared 18Aβ group to 3Vh and 3Aβ groups, and to 18Vh. In this way, it was possible to highlight the role of aging process (18Aβ vs. 3Aβ), the role of $A\beta_{1-42}$ oligomers in elderly (18Aβ vs. 18Vh) and both the conditions (18Aβ vs. 3Vh). RNA-seq data were generated and revealed 21,769 differentially expressed genes for the analysis 18Aβ vs. 3Aβ (up 7095 and down 14674), 19,600 for the analysis 18Aβ vs. 18Vh (up 8867 and down 10735), and 22,466 for the analysis 18Aβ vs. 3Vh (up 7690 and down 14776).

Expression data were analyzed for enrichment analysis by GSEA using parameters recommended for expression datasets with less than 7 replicates for samples: datasets were converted into gene symbols, redundant probe sets were collapsed using probe medians, a Signal2Noise metric was used for ranking genes, and the weighted enrichment statistic and 1000 gene set permutations were employed. Table II shows the summary of up-regulated and down-regulated genes for each analysis performed.

Table II. Summary of up- and down-regulated genes in GSEA analysis

		3Vh	3Aβ	18Vh
18Aβ	UP	3946	848	3032
	DOWN	450	57	1185

The heatmaps representing the most dysregulated genes are shown in Figure 11 for each analysis carried out.

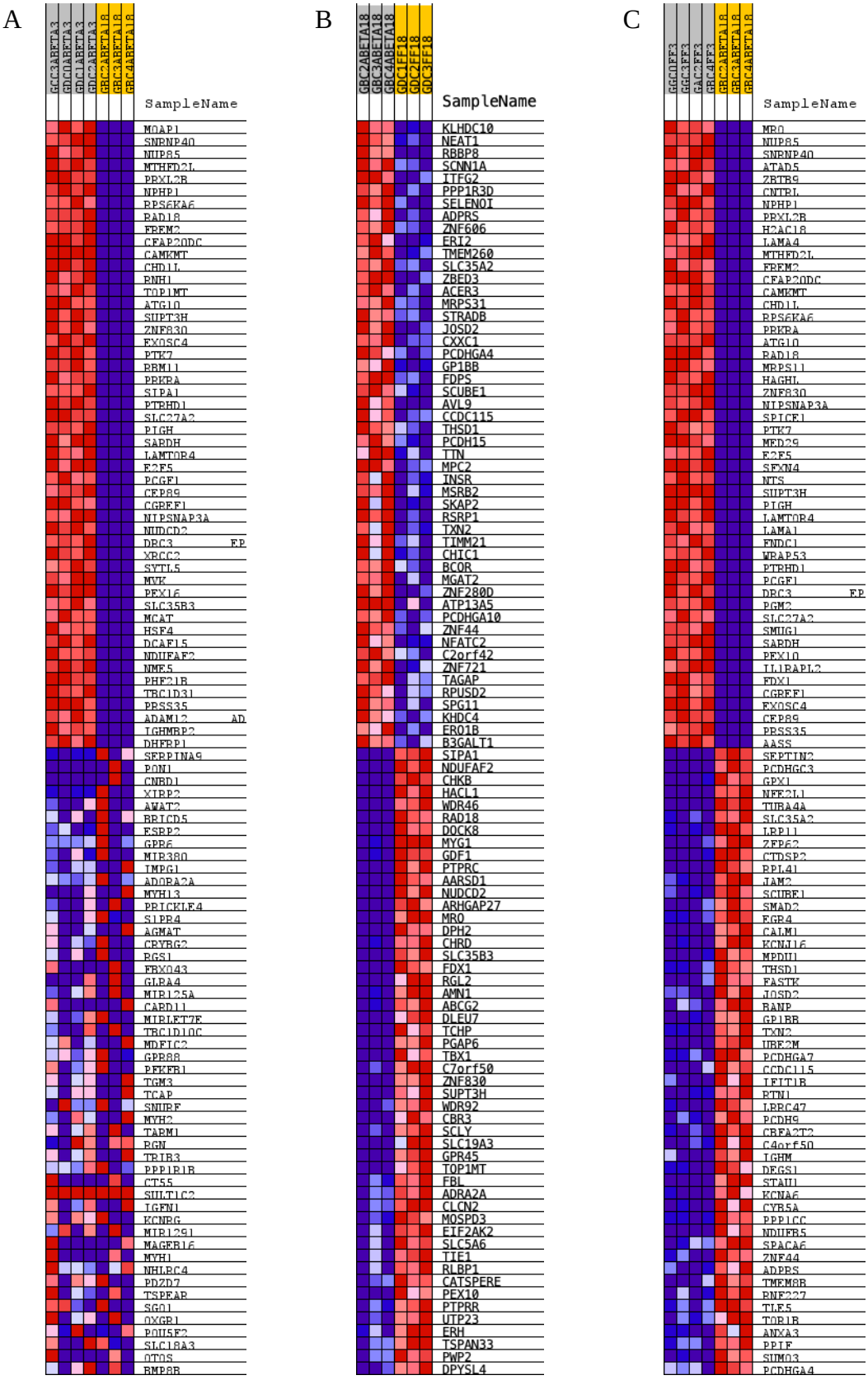

Figure 11. Heatmaps representing the most dysregulated genes in the analysis 18Aβ vs. 3Aβ (A), 18Aβ vs. 18Vh (B), and 18Aβ vs. 3Vh (C) generated with GSEA. Expression values are represented as colors and range from red (high expression), pink (moderate), light blue (low) to dark blue (lowest expression).

GSEA revealed that genes linked to mTOR (Fig 12A-B, 12D-E) and ERK signaling pathways (Fig. 12C and 12F) were enriched in 3Aβ.

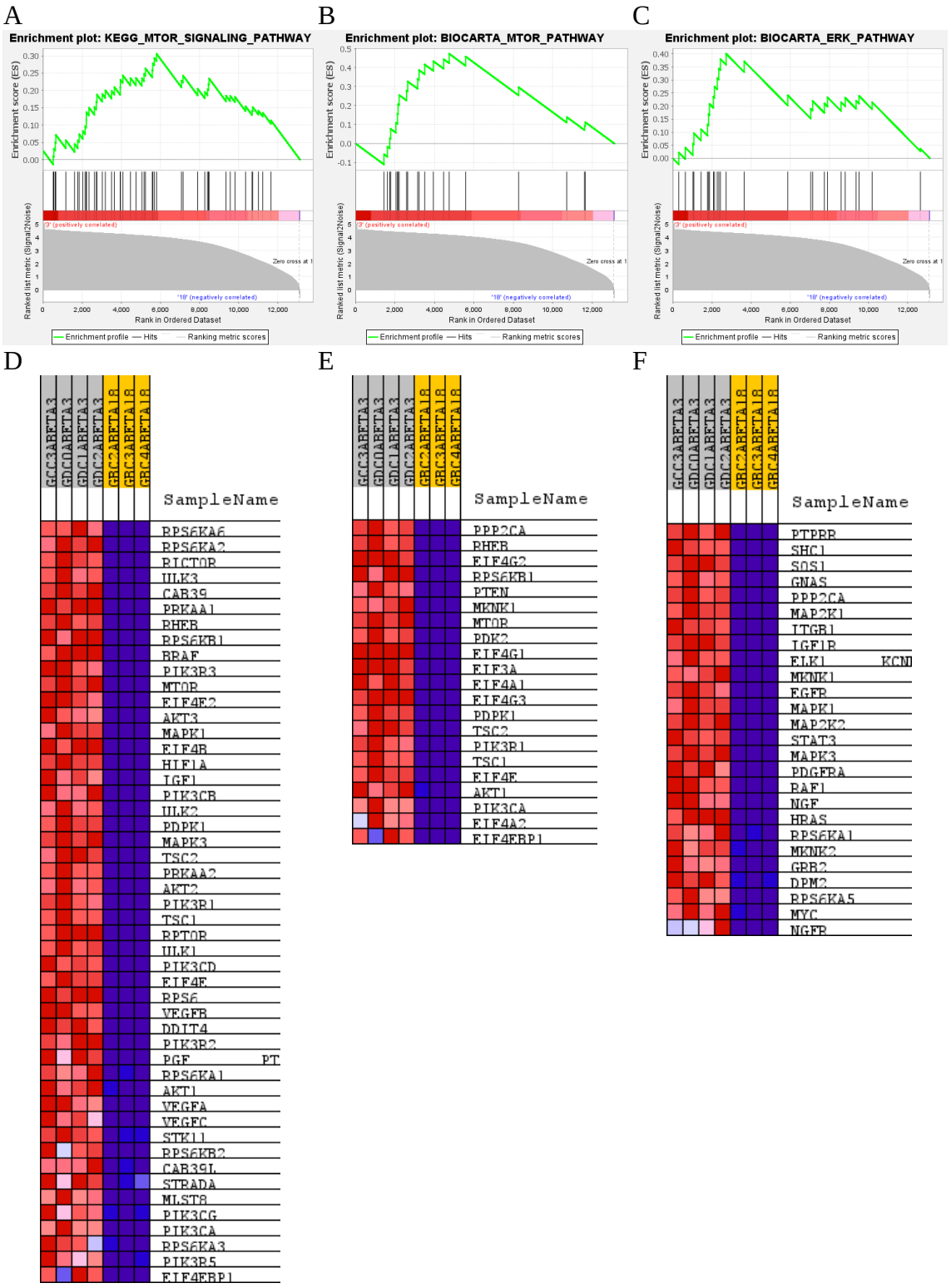

Figure 12. Enrichment plots (A-C) and heat maps (D-F) for core enrichment genes were generated by GSEA using the KEGG (A and D), BIOCARTA (B and E), and (C and F) gene sets. Comparison identified the enrichment of the "mTOR signaling pathway", "mTOR pathway" and "ERK pathway" gene sets in 3Aβ compared to 18Aβ. Expression values are represented as colors and range from red (high expression), pink (moderate), light blue (low) to dark blue (lowest expression).

The same analysis conducted with TOPPGENE highlighted the up-regulation of phenotypes “increased inflammatory response” (HP: 0012649; p-value 0.00009; FDR 0.128) and “abnormal inflammatory response” (HP: 0012647; p-value 0.00009; FDR 0.128), and the upregulation of the pathway “diseases associated with the TLR signaling cascade” (Reactome: 1269157; p-value 0.000003; FDR 0.0008) in 3Aβ group as compared to 18Aβ group. Interestingly, the analysis showed up-regulation of genes involved in “neurodegenerative disorders” (DisGeNET: C0524851; p-value 0.00067; FDR 0.3) in 18Aβ group.

The GSEA analysis in healthy and lesioned aged animals (18Vh vs. 18Aβ) highlighted that genes linked to oxidative stress (Fig. 13) were enriched in 18Aβ.

A B

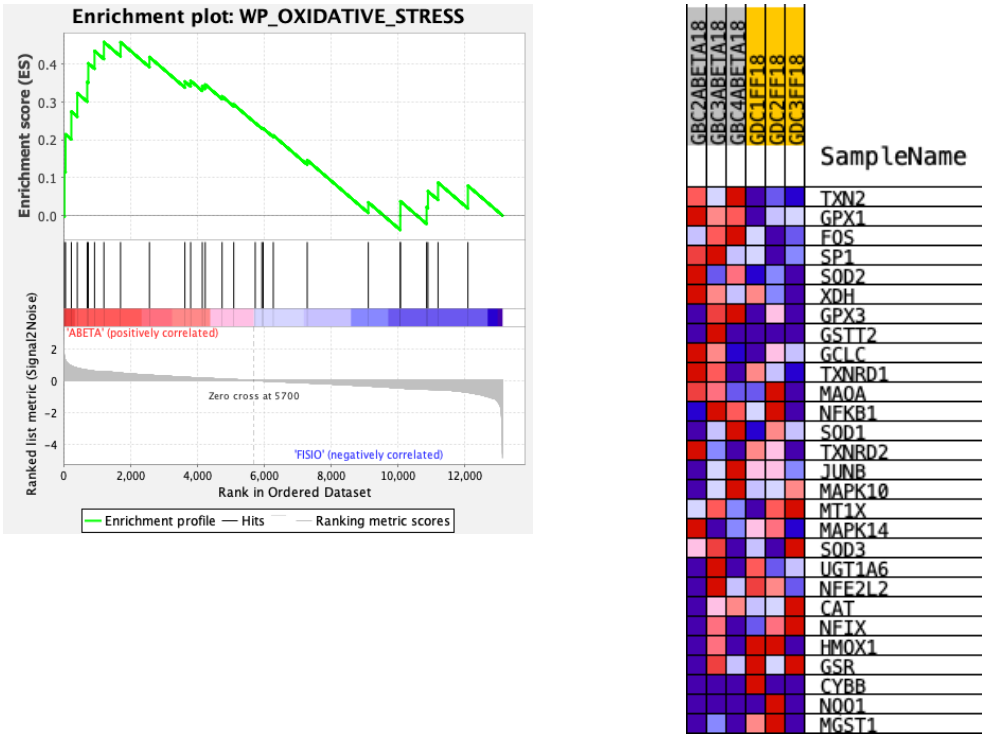

Figure 13. Enrichment plots (A) and heat maps (B) for core enrichment genes were generated by GSEA using the WP gene set. Comparison identified the enrichment of the “oxidative stress” gene set in 18Aβ compared to 18Vh. Expression values are represented as colors and range from red (high expression), pink (moderate), light blue (low) to dark blue (lowest expression).

Finally, GSEA analysis for the comparison between 3Vh and 18Aβ animals showed the dysregulation of several pathways, as oxidative phosphorylation and Ras pathway (Fig. 14), aging and AD (Fig. 15), and ER regulation (Fig. 16).

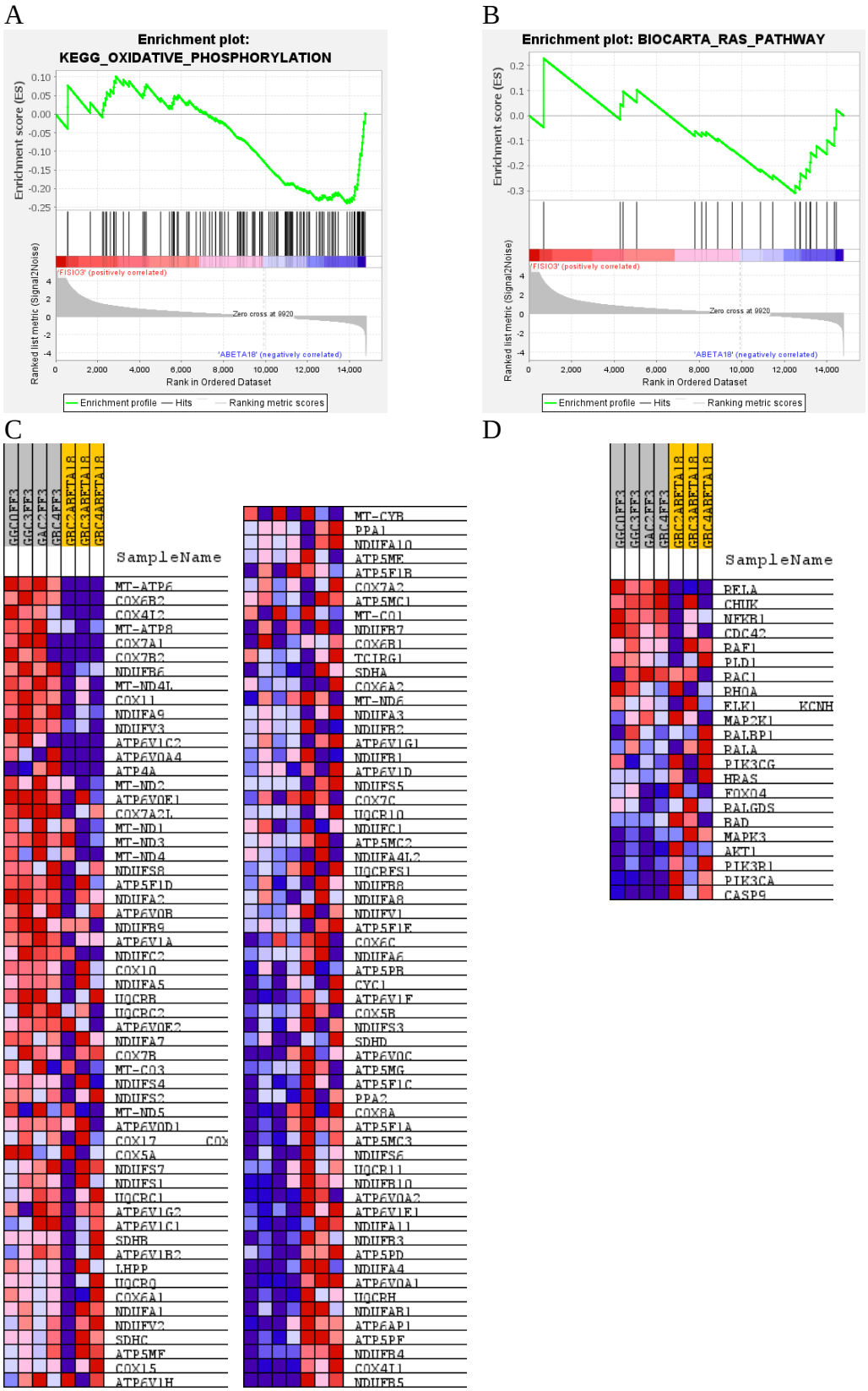

Figure 14. Enrichment plots (A-B) and heat maps (C-D) for core enrichment genes were generated by GSEA using the KEGG (A and C), BIOCARTA (B and D) gene sets. Comparison identified the enrichment of the "oxidative phosphorylation", and "Ras pathway" gene sets in 18Aβ compared to 3Vh. Expression values are represented as colors and range from red (high expression), pink (moderate), light blue (low) to dark blue (lowest expression).

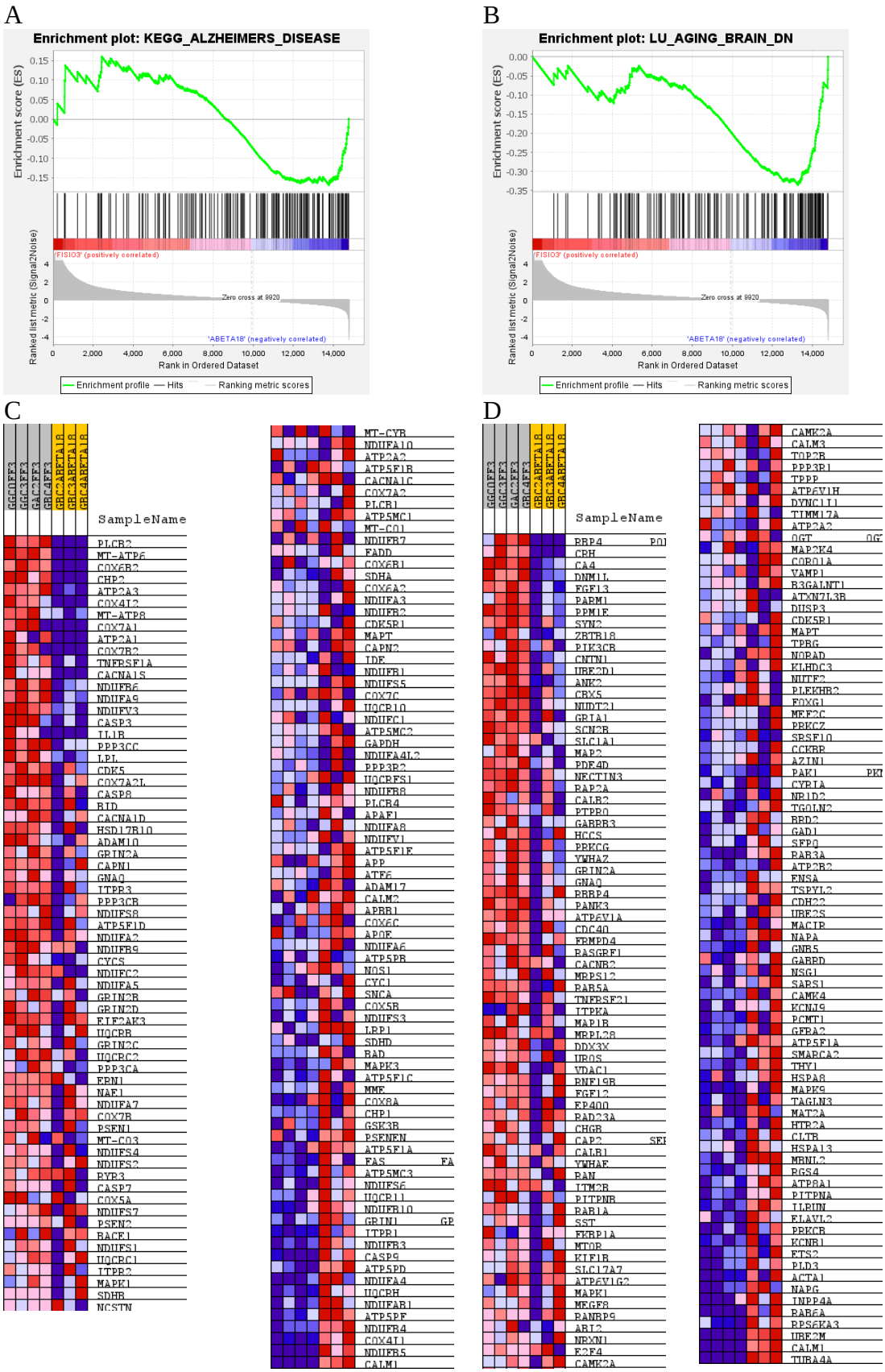

Figure 15. Enrichment plots (A-B) and heat maps (C-D) for core enrichment genes were generated by GSEA using the KEGG (A and B), LU (B and D) gene sets. Comparison identified the enrichment of the "Alzheimer's disease", and "aging brain" gene sets in 18Aβ compared to 3Vh. Expression values are represented as colors and range from red (high expression), pink (moderate), light blue (low) to dark blue (lowest expression).

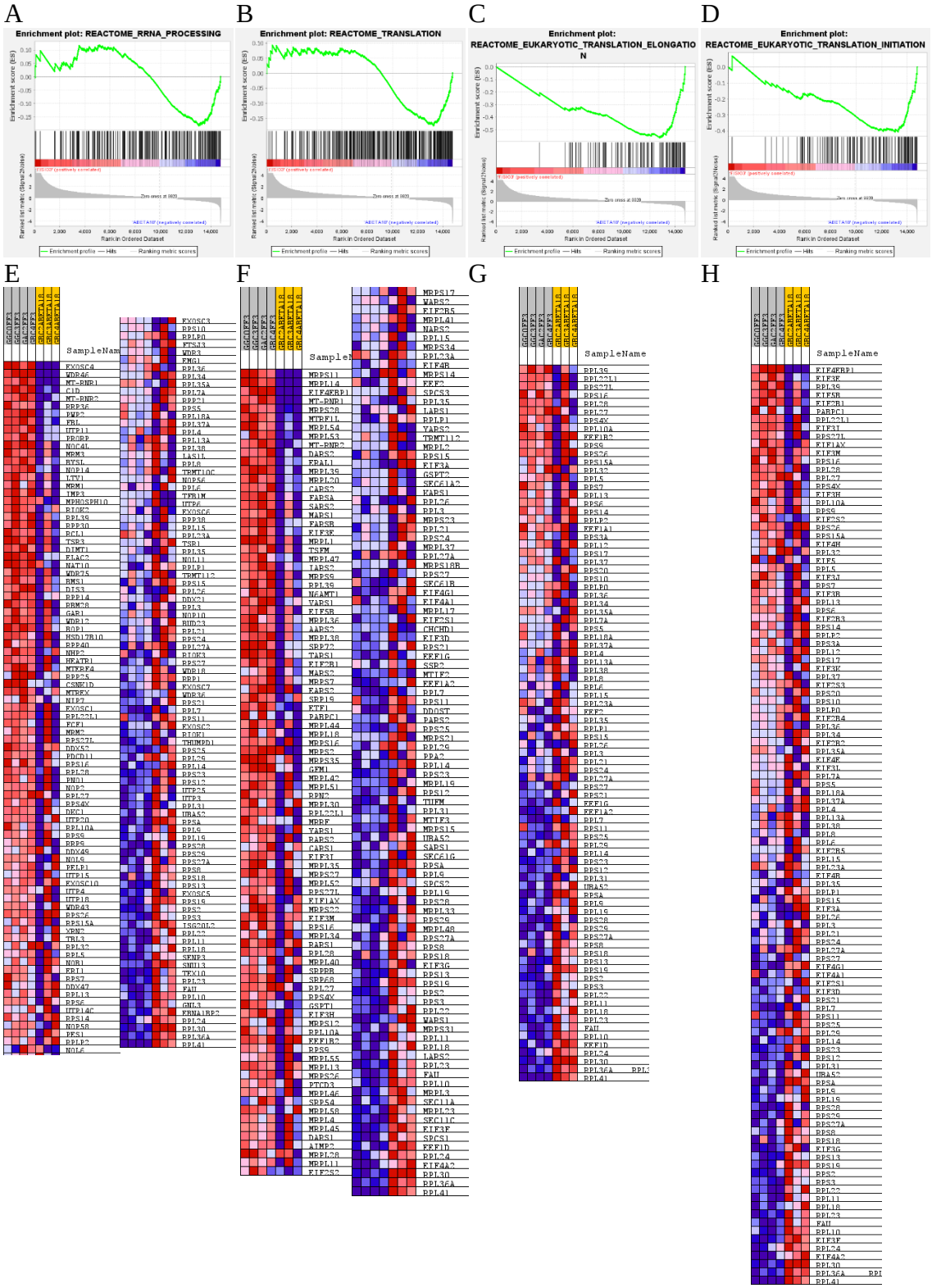

Figure 16. Enrichment plots (A-D) and heat maps (E-H) for core enrichment genes were generated by GSEA using the REACTOME gene sets. Comparison identified the enrichment of the "RRNA processing", "translation", "eukaryotic translation elongation", and "eukaryotic translation initiation" gene sets in 18Aβ compared to 3Vh. Expression values are represented as colors and range from red (high expression), pink (moderate), light blue (low) to dark blue (lowest expression).

The expression data obtained from the sequencing were analyzed and filtered using as a cutoff p-adjusted of < 0.05 and -2 < log2(FC) > 2. From the moment that the number of counts was not high for 18Vh and 18Aβ groups, in the comparison between these two experimental groups we used a p-value < 0.05 as a cutoff. Indeed, with aging our samples showed a minor content/quality of RNA that indicates a poor outcome for the proteostasis network. We then used volcano plots to visualize the distribution of significantly dysregulated genes in all comparison performed (Fig. 17A-C).

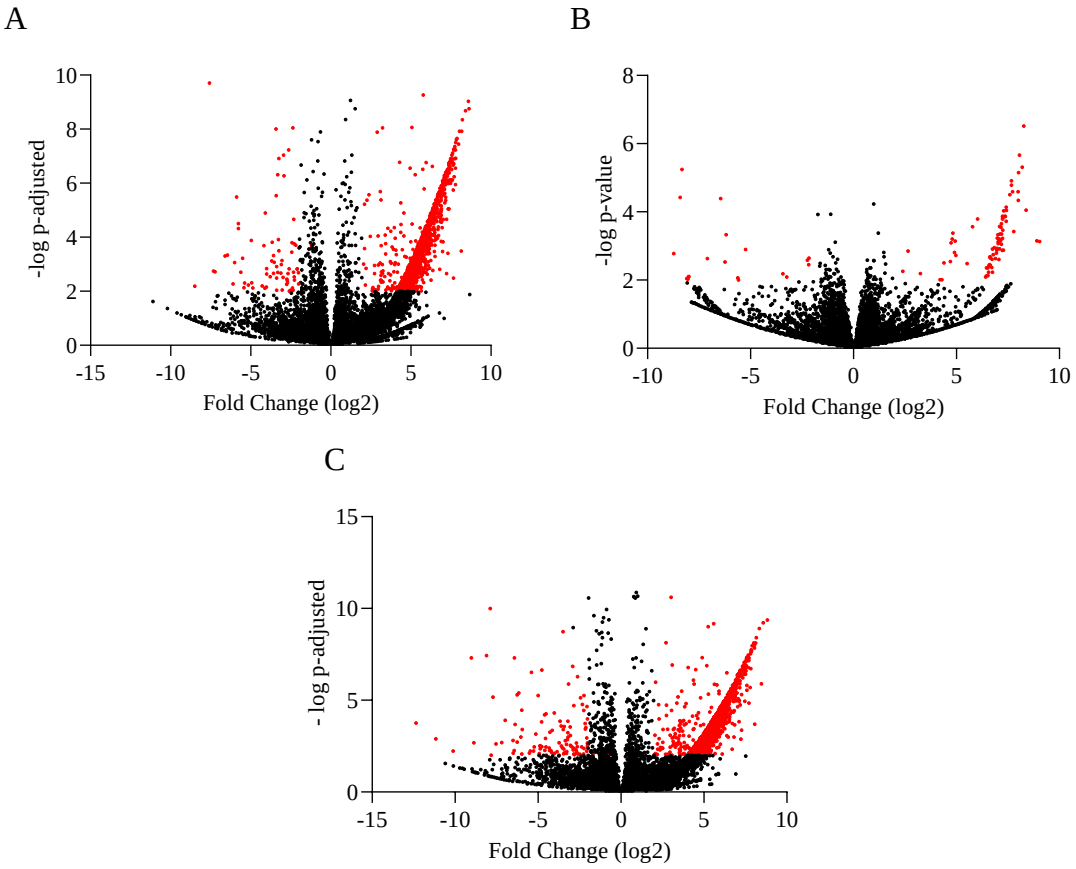

Figure 17. Volcano plot of significant dysregulated genes in comparison 18Aβ vs. 3Aβ (A), 18Aβ vs. 18Vh (B), and 18Aβ vs. 3Vh (C). The Volcano plot indicates -log 10 (p-adjusted or p-value) for genome-wide genes (Y-axis) plotted against their respective log 2 (fold change) (X-axis). The red dots represent significantly up-and down-regulated genes.

After that we conducted a gene ontology (GO) analysis with software GOrilla on the significantly dysregulated genes in all three comparisons. Significantly dysregulated biological processes are show for comparison 18Aβ vs. 3Aβ (Fig. 18), for the analysis 18Aβ vs. 18Vh (Fig. 19), and for 18Aβ vs. 3Vh (Fig. 20).

The first analysis highlighted the significant dysregulation of GO terms involved in the "regulation protein kinase activity", "proteolysis", "protein glycosylation", "detoxication" ($10^{-3} < p < 10^{-5}$), and "cellular process" ($10^{-5} < p < 10^{-7}$).

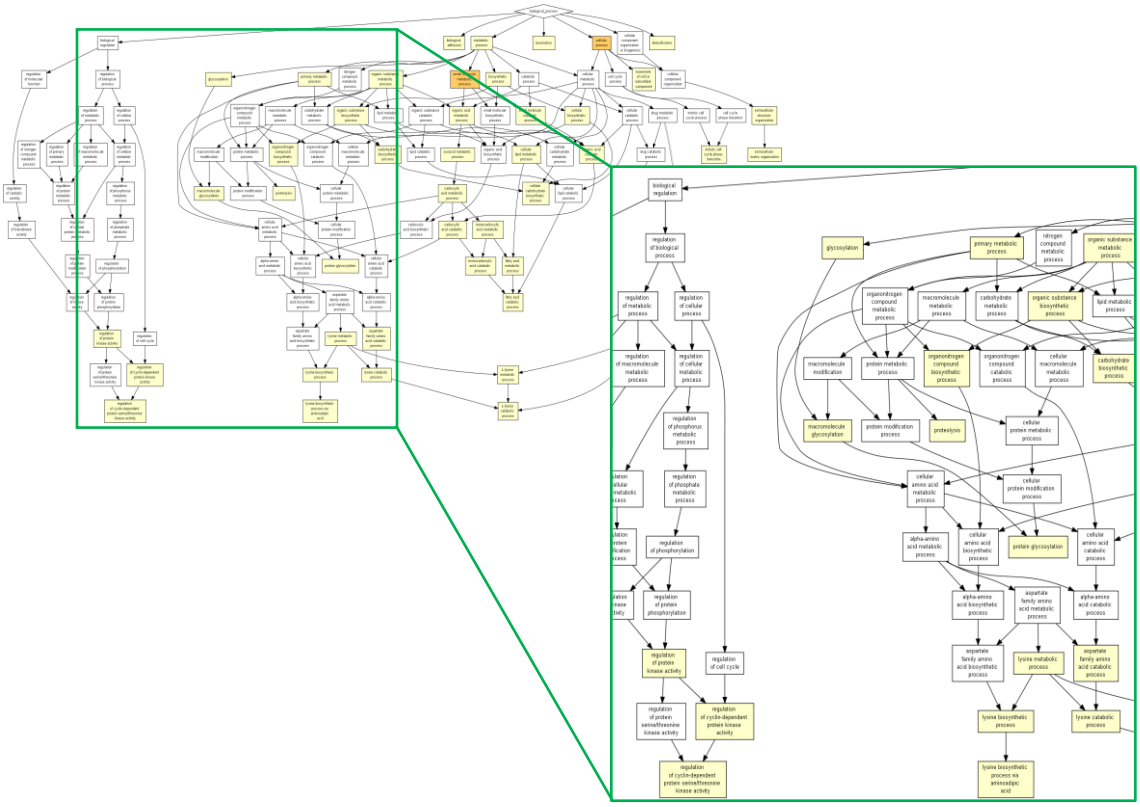

Figure 18. GOrilla reveals the GO terms in Process gene ontology domains, enriched with genes differentially expressed in 18Aβ when compared to 3Aβ. The pathways analysis was conducted at on 1273 differentially expressed genes ($p < 0.05$). Yellow squares represent the GO terms with $10^{-3} < p < 10^{-5}$, orange squares represent $10^{-5} < p < 10^{-7}$.

The second analysis (Fig. 19) conducted on the comparison between 18Vh and 18Aβ showed the involvement of GO terms related to "proteolysis" and "regulation of system process" ($10^{-3} < p < 10^{-5}$).

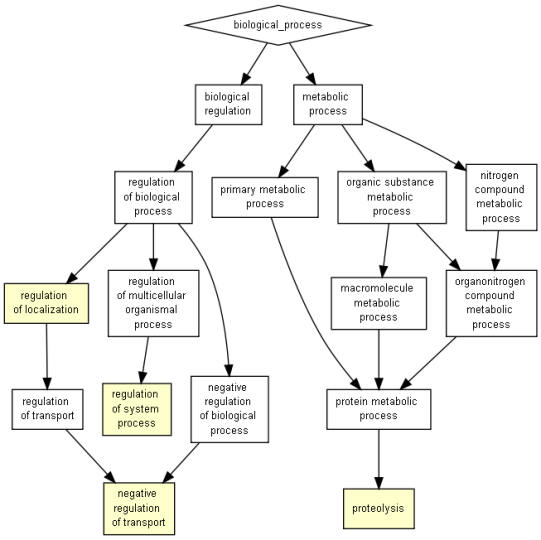

Figure 19. GOrilla reveals the GO terms in Process gene ontology domains, enriched with genes differentially expressed in 18Aβ when compared to 18Vh. The pathways analysis was conducted at on 182 differentially expressed genes ($p < 0.05$). Yellow squares represent the GO terms with $10^{-3} < p < 10^{-5}$.

Finally, the analysis between healthy young animals as compared to old, lesioned mice (Fig. 20) showed again the dysregulation of “regulation protein kinase activity”, “proteolysis”, “detoxication” and “intrinsic apoptotic signaling pathways in response to endoplasmic reticulum stress” ($10^{-3} < p < 10^{-5}$).

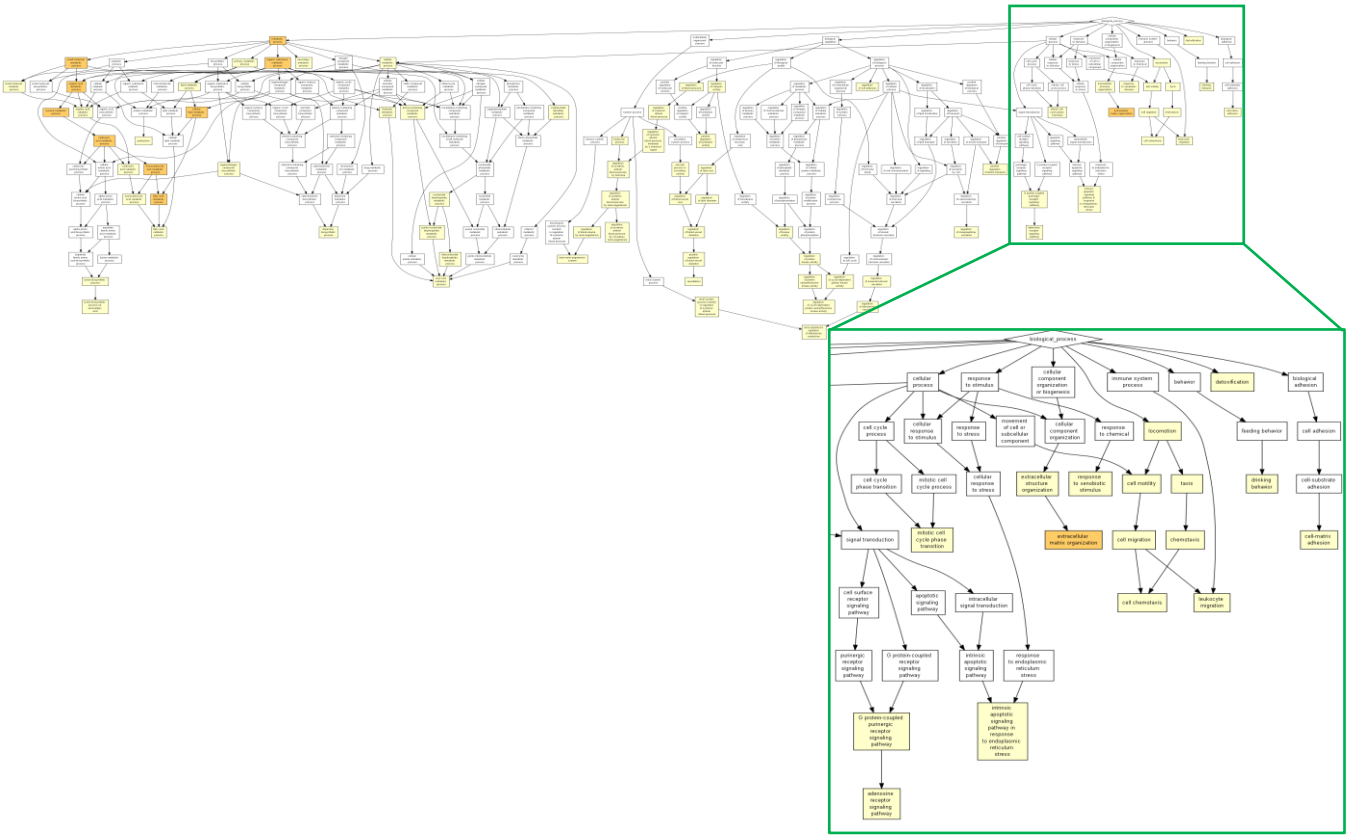

Figure 20. GOrilla reveals the GO terms in Process gene ontology domains, enriched with genes differentially expressed in 18Aβ when compared to 3Vh. The pathways analysis was conducted at on 1605 differentially expressed genes ($p < 0.05$). Yellow squares represent the GO terms with $10^{-3} < p < 10^{-5}$, orange squares represent $10^{-5} < p < 10^{-7}$.

After that, we designed a Vienn diagram among all significantly dysregulated genes, and we observed that 125 genes were shared by all the comparisons conducted (Fig. 21). On the contrary, healthy and lesioned old mice shared only 3 genes with young and old lesioned mice, as well as 7 with healthy young and old lesioned. The two comparisons which share the largest number of significantly dysregulated genes are young and old lesioned, and young healthy and old lesioned.

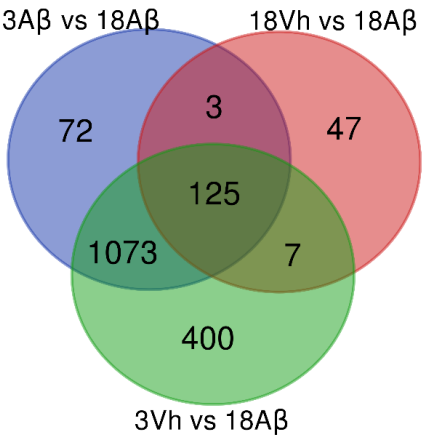

Figure 21. Venn diagram of the differentially significantly expressed genes. The number in each circle represents the amount of differentially expressed genes between the different comparisons. The overlapping number stands for the mutual differentially expressed genes between the different comparisons and the non-overlapping numbers specify the genes unique to each condition.

Thus, an analysis with PANTHER was conducted only on the 125 dysregulated genes. Figure 22 shows that among the biological process (A) associated to dysregulated genes there is also "transcription regulator activity" (GO:0140110), "molecular function regulator" (GO:0098772), and among the pathways (B) highlighted by the analysis we found "Alzheimer's disease-presenilin pathway" (P:00004), "Apoptosis signaling pathway" (P:00006), and "Inflammation mediated by chemokine and cytokine signaling pathway" (P:00031).

We analyzed all the genes involved in the significantly highlighted process obtained by the GOrilla analysis ($10^{-3} < p < 10^{-7}$) and we observed that all GO term showed the involvement of at least one gene of the 125 significantly dysregulated among all comparisons. Among the 125 significantly dysregulated genes, 68 were highlighted by GO term analysis and summarized in Table III.

Table III. Significantly dysregulated genes in GOrilla analysis and common to all comparisons

Abcg2	Chkb	Eme2	Haghl	Mapkapk5	Nudcd2	Polr3b
Ahr	Chrd	Exosc4	Hfe	Mboat1	Nup85	Prpsap2
Alkbh7	Csgalnact2	Fancg	Id1	Mcm7	Parp9	Psmg2
Amn1	Dcxr	Fcgr1	Ifi203	Moap1	Pedh20	Ptprc
Ap5z1	Dhodh	Fdx1	Igtp	Mospd3	Pcdha2	Ptprr
Arhgap25	Dhps	Fn3k	Kcns1	Myd88	Pex10	Rad18
Arghap27	Dock2	Fuz	Kif11	Ncf2	Pigh	Rbm11
B4galt1	Dock8	Gp1bb	Lamtor4	Ndufaf2	Pigx	Sardh
Cbr3	Dph2	Gstm4	Lbp	Nostrin	Plcd3	
Ccnf	Ehbp1l1	Hacl1	Lsm7	Nphp1	Plk5	

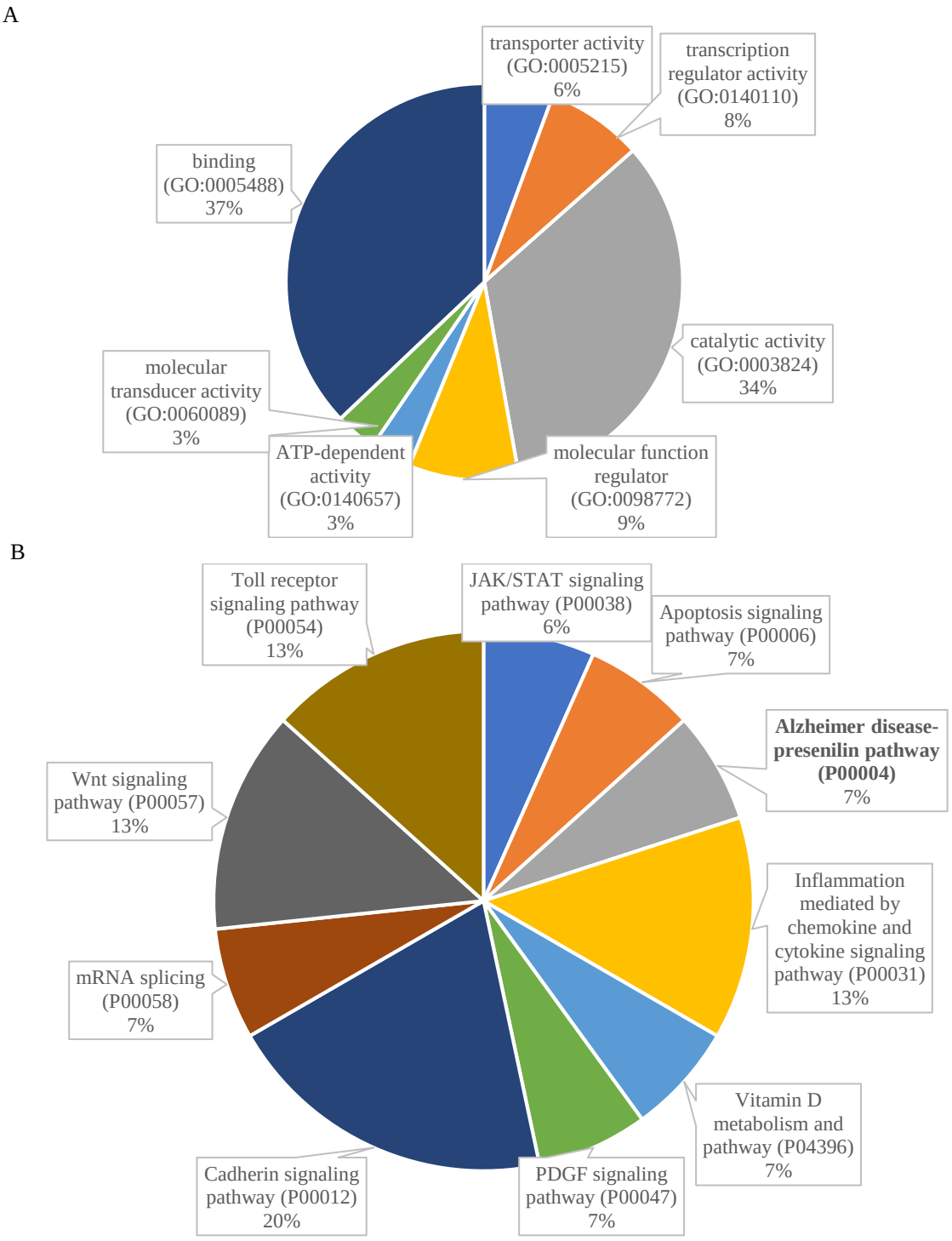

Figure 22. Gene classification pie charts created in PANTHER. Biological process (A) and pathways (B) associated to common 125 dysregulated genes in comparisons 18Aβ vs. 3Aβ, 18Aβ vs. 18Vh, and for 18Aβ vs. 3Vh.

Among the 68 selected genes, the dysregulation of gene Mapkapk5 is summarized in Table IV. The analysis shows that Mapkapk5 is significantly up-regulated in healthy young mice and its expression declines after the lesion induced by i.c.v. injection with $A\beta_{1\text{-}42}$ oligomers and with aging.

Table IV. Gene expression of Mapkapk5 in all comparisons conducted

3Aβ vs. 18Aβ	**Log2FoldChange**	**p-value**	**p-adj**
	5.975	$1.17e^{-6}$	$6.00e^{-5}$
18Vh vs. 18Aβ	**Log2FoldChange**	**p-value**	**p-adj**
	5.522	0.003	0.674
3Vh vs. 18Aβ	**Log2FoldChange**	**p-value**	**p-adj**
	6.384	$1.94e^{-9}$	$3.18e^{-7}$

After the bioinformatic analysis, we investigated the cellular redox status through the evaluation of ROS formation (Fig. 23A) and GSH levels (Fig. 23B). Results show a significant increase in the ROS formation after the $A\beta_{1-42}$ oligomers injection in both young and aged animals as compared to the respective healthy group. Moreover, GSH levels decrease significantly both with aging and after the lesion induced.

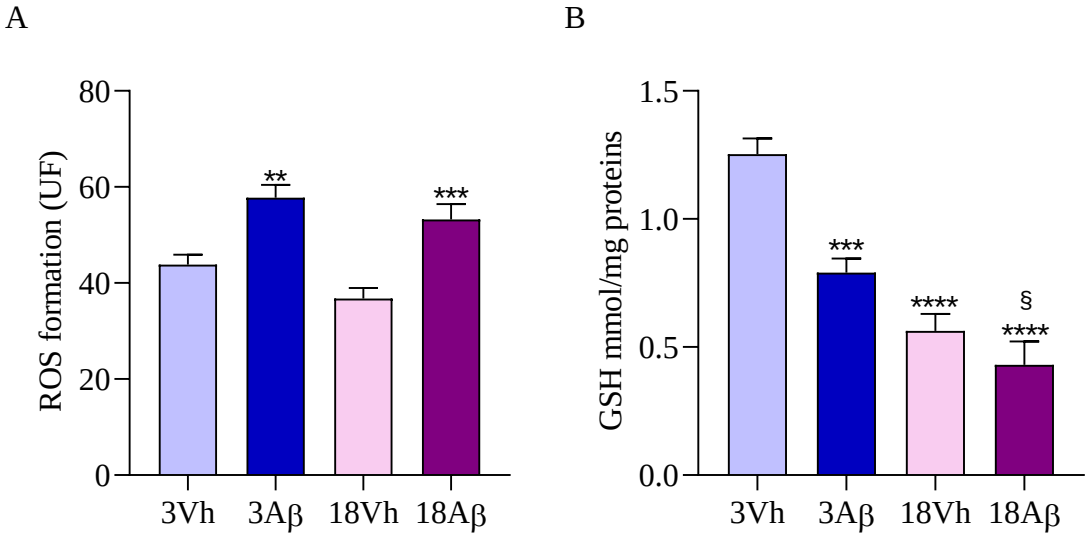

Figure 23. Effects of i.c.v. injection with $A\beta_{1-42}$ oligomers in young and aged mice on cellular redox status. ROS formation was evaluated in the hippocampal samples based on DCF's fluorescence emission at 535 nm after excitation at 485 nm. The values are expressed as mean ± SEM (n = 7) of fluorescence intensity arbitrary units (UF) of each experimental group (A). GSH content was measured using a colorimetric assay in the hippocampal samples. The values are calculated using a standard calibration curve and expressed as mean ± SEM (n = 10) of mmol GSH/mg protein (B) (A: **p < 0.01 vs. 3Vh group, ***p < 0.001 vs.18Vh group; B: ***p < 0.001 and ****p < 0.0001 vs. 3Vh group, §p < 0.05 vs. 3Aβ group; one-way ANOVA, post hoc test Tukey).

To better understand the involvement of the pathways highlighted by the enrichment analysis, we analyzed protein expression levels by Western Blotting. Firstly, we evaluated protein involved in the UPR and in ER stress. Figure 24 shows the activation of the three pathways involved in the ER stress: PERK/p-eIF2α (Fig. 24A-B), IRE1α (C), and ATF-6 (D) in aged and lesioned mice. In particular, the activation of PERK/p-eIF2α pathway is significant in 18Aβ mice, while IRE1α shows an increase in 3Aβ mice, which

becomes significant in aged healthy and lesioned animals. Moreover, ATF-6 shows a significant decrease in its activation related to the treatment but not to the age of the group.

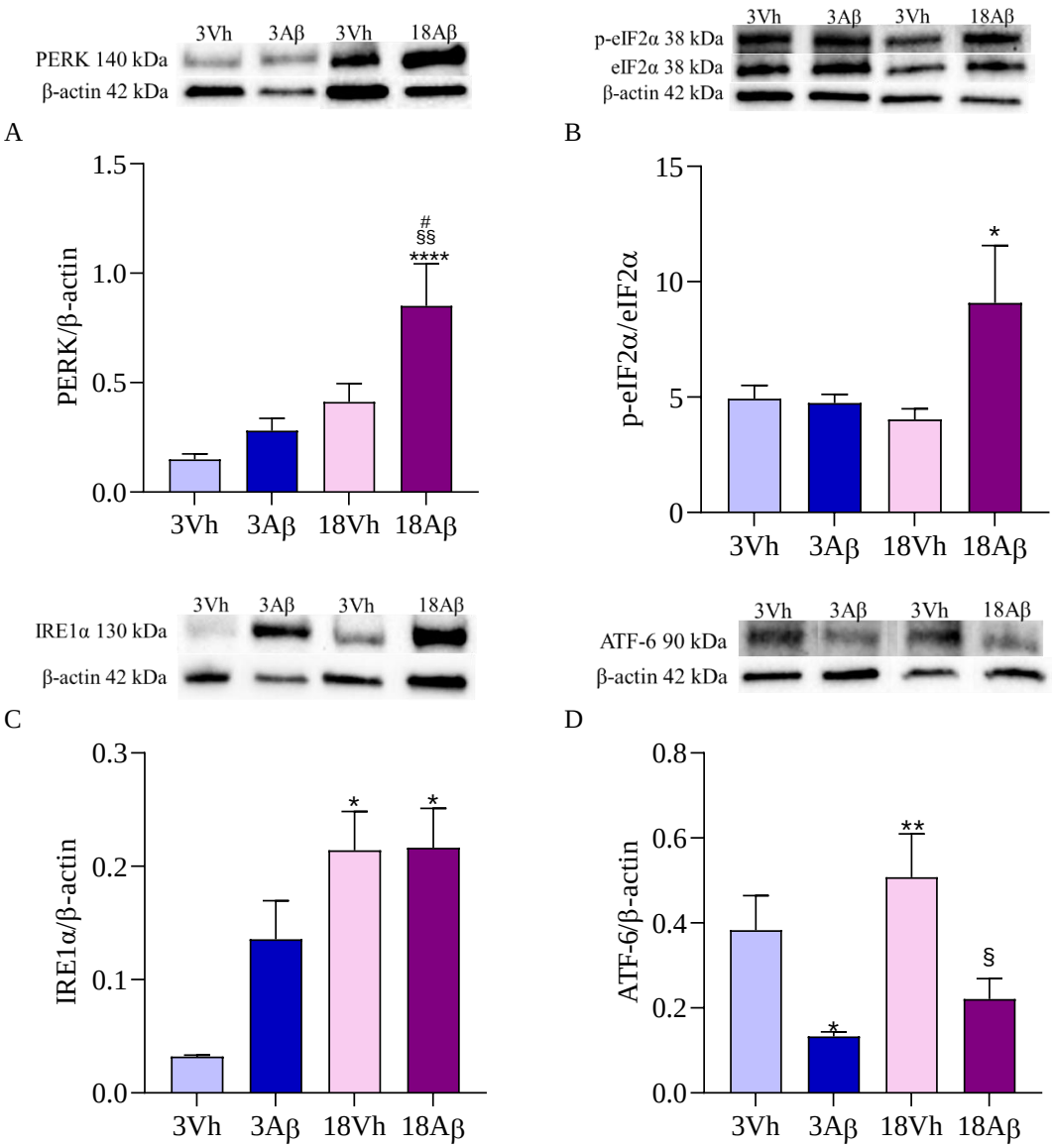

Figure 24. Effects of i.c.v. injection with $A\beta_{1\text{-}42}$ oligomers in young and aged mice on PERK (A), p-eIF2α (B), IRE1α (C), and ATF-6 (D). PERK, p-eIF2α, IRE1α, and ATF-6 were determined by Western blotting in the hippocampal samples at 140, 38, 130, and 90 kDa, respectively, and using total eIF2α, and β-actin (42 kDa) as loading control. Top: representative images of PERK and β-actin (A); p-eIF2α, eIF2α and β-actin (B); IRE1α and β-actin (C), ATF-6 and β-actin (D) expressions. Bottom: quantitative analysis of the Western blotting results for the PERK (A), p-eIF2α (B), IRE1α (C), and ATF-6 levels. The graphs show densitometry analysis of the bands appertaining to the protein of interest. The values are expressed as mean ± SEM (n = 7) of each group. (A: $^{\#}p < 0.05$ vs. 18Vh group, $^{\S\S}p < 0.01$ vs. 3Aβ, and ****$p < 0.0001$ vs. 3Vh group; B: *$p < 0.05$ vs. 3Vh, 3Aβ, and 18Vh groups; C: *$p < 0.05$ vs. 3Vh group; D: *$p < 0.05$ vs. 3Vh group, **$p < 0.01$ vs. 3Aβ group, and $^{\S}p < 0.05$ vs. 18Vh group; one-way ANOVA, post hoc test Tukey).

Finally, we investigated the involvement of the phosphatidylinositide-3-OH kinase (PI3K)/Akt and MAPK/ERK pathways in our model of AD through the phosphorylation of Akt, GSK3β, p-ERK, and Mapkapk5 (Fig.25). Our results show a significant decrease in the phosphorylation of Akt in aged animals (both lesioned and healthy; Fig. 25A), and

GSK3β which correspond to a significant increase of activity of this kinase (Fig. 25B). Moreover, we observed a significant decrease in the phosphorylation of ERK 1/2 in 18Vh and 18Aβ groups as compared to 3Vh and 3Aβ groups, and a tendency to decrease, but not significant, in Mapkapk5 activation in the same experimental groups (Fig. 25C-D).

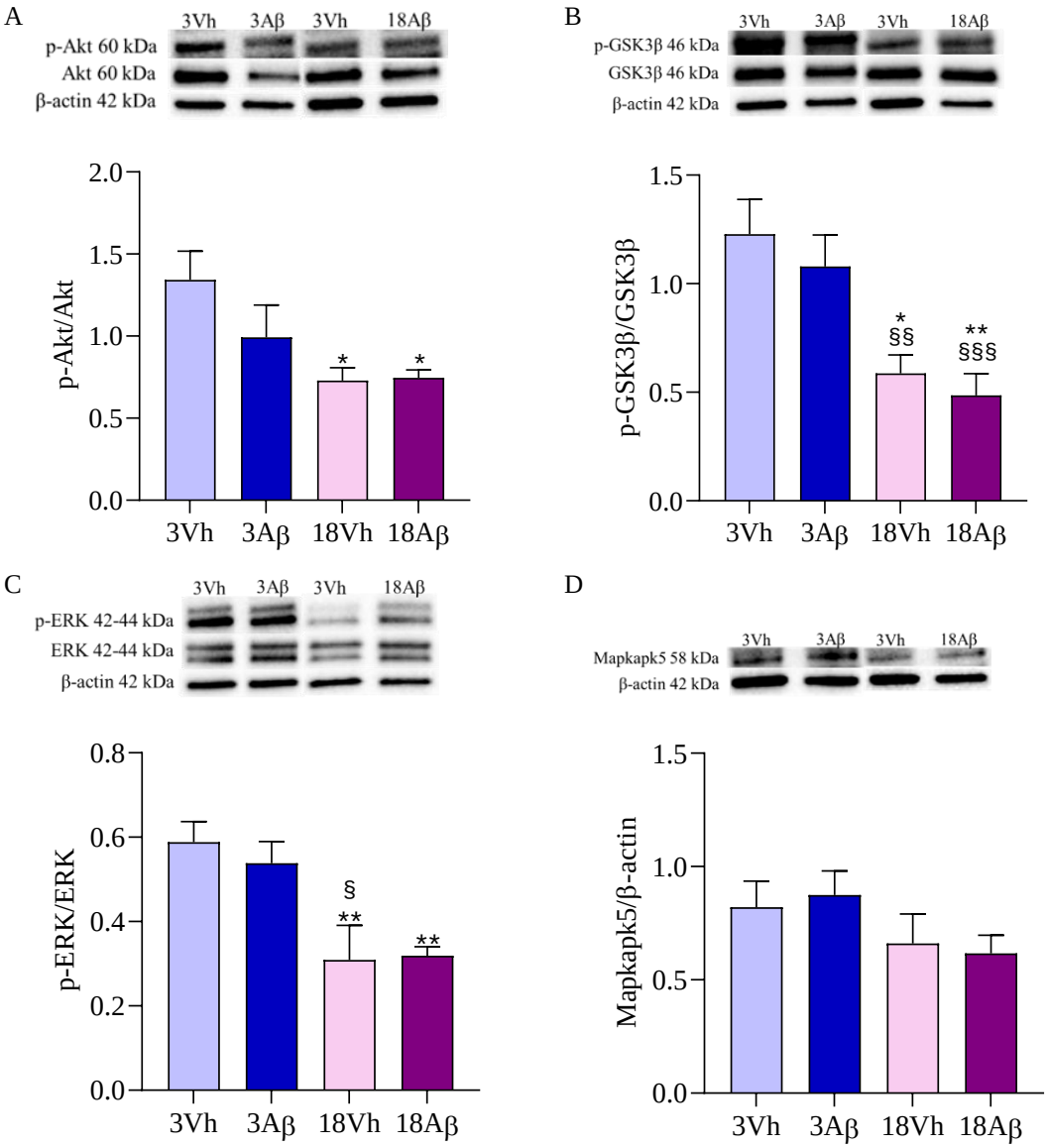

Figure 25. Effects of i.c.v. injection with $A\beta_{1-42}$ oligomers in young and aged mice on p-Akt (A), p-GSK3β (B), p-ERK (C), and Mapkapk5 (D). p-Akt, p-GSK3β, p-ERK, and Mapkapk5 were determined by Western blotting in the hippocampal samples at 60, 46, 42/44, and 58 kDa, respectively, and using Akt, GSK3β, ERK and β-actin (42 kDa) as loading control. Top: representative images of p-Akt, Akt, and β-actin (A), p-GSK3β, GSK3, and β-actin (B), p-ERK, ERK, and β-actin (c), and Mapkapk5 and β-actin (D) expressions. Bottom: quantitative analysis of the Western blotting results for the p-Akt (A), p-GSK3β (B), p-ERK (C), and Mapkapk5 (D) levels. (A: *$p < 0.05$ vs. 3Vh group; B: $^{§§}p < 0.01$ and $^{§§§}p < 0.001$ vs. 3Vh group, *$p < 0.05$ and **$p < 0.01$ vs. 3Aβ group; C: $^{§}p < 0.05$ vs. 3Aβ group, **$p < 0.01$ vs. 3Vh group; one-way ANOVA, post hoc test Tukey).

5. DISCUSSION

AD is a multifaced neurodegenerative disease which represents the leading cause of dementia worldwide. The first risk factor for AD is the aging process and the related involvement of the neuroinflammatory response, the decline of antioxidative resources, and the increasing accumulation of misfolded proteins due to the failure of the UPR. In the present study, the role of the aging process was evaluated in a mice model of AD induced by i.c.v. injection of $A\beta_{1-42}$ oligomers in young and aged mice (3 and 18 months).

According to our current knowledge, there is still no animal model with all the cognitive, behavioral, biochemical and histopathological abnormalities that characterize AD. Several studies have demonstrated that i.c.v. injection with $A\beta_{1–42}$ to mice could induce significant neuron death, inflammatory response and memory impairments[42]. Growing evidence indicates that Aβ-injected rodent models of AD might closely mimic the main neuropathological symptoms present in AD patients when concentrations of Aβ are increasing[43]. Many studies have reported behavioral and neurochemical consequences obtained after i.c.v. injection of the $A\beta_{1-42}$ peptide. The most widely used dose is 400 pmol, but we decided to inject 6 µL of Abeta 40 µM, which is about 1 µg or 240 pmol of oligomeric Aβ, a much lower dose (240 pmol), trying to assess the early effects of Aβ oligomers. Similarly, Chiba et al. demonstrated that injection of 300 pmol of $A\beta_{1-42}$ significantly induced memory impairment at a week post-injection[169]. Moreover, 200 pg of Aβ peptide is the approximate quantity of Aβ in a single amyloid plaque in AD brain[44].

The cognitive impairment was firstly investigated by behavioral assessment using Y-maze and Morris water maze tests. According to Yang et al., results obtained showed a significant impairment after the lesion induced in old mice as compared to younger animals[170]. The older and healthy experimental group did not show a significant alteration

to the learning and mnesic capacities as compared to younger mice. This result indicate that $A\beta_{1-42}$ oligomers injection induces a different output according to the age of animals.

Gene expression analysis and gene set enrichment analysis showed the dysregulation of different pathways in the comparisons performed, highlighting the involvement of the oxidative response, PI3K/Akt/mTOR and ERK pathways, and alterations at ER level. Interestingly, the enrichment analysis of the comparison between 18Aβ and 3Vh (up 3946 and down 450) showed dysregulation of genes involved in pathways related to AD and the aging process.

The following analysis on the GO terms conducted on significant dysregulated genes confirmed the involvement of ER and the regulation of protein kinase activity. The three comparisons conducted (18Aβ vs. 18Vh, 18Aβ vs. 3Aβ, 18Aβ vs. 3Vh) showed the significant dysregulation of 125 common genes to all the analysis and, among these, 68 involved in the pathways highlighted by the GO terms analysis. Moreover, gene classification conducted on PANTHER highlighted again the involvement of "Alzheimer's disease pathway".

Following the bioinformatic analysis, biomolecular assessment was performed to evaluate the cellular redox status. According to Leutner et al., the aging process did not affect ROS production in hippocampal samples as compared to healthy young mice[171]. After the lesion with $A\beta_{1-42}$ oligomers, a significant increase of ROS production was recorded both in young and aged mice[42]. On the contrary, several studies have shown that GSH levels decrease after the treatment with $A\beta_{1-42}$ oligomers and during aging[172–174]. Our results confirm this hypothesis and suggest that the increased susceptibility of the aging and AD brain to oxidative damage may be a consequence of GSH depletion.

The involvement of ER stress and UPR highlighted by the enrichment analysis was then investigated by Western Blotting. Several studies have reported that ER stress is a common pathological feature of AD[140]. Indeed, UPR activation has been observed in postmortem AD brain, indicating a correlation between the presence of hyperphosphorylated Tau and ER stress markers in cortical neurons[139]. Moreover, studies in cell culture models of AD suggest that ER stress mediates in part the occurrence of neuronal loss triggered by Aβ[175]. Remarkably, human neurons derived from induced pluripotent stem cells of AD patients revealed that ER stress is a prominent feature of this disease model[176]. Importantly, the well-known effects of UPR signaling on protein translation repression were shown to contribute to the cognitive impairment observed in AD models involving activation of the stress sensor PERK and the phosphorylation of

the protein translation initiation factor eIF2α[177]. UPR is triggered by three main branches: the axes PERK/p-eIF2α, IRE1α, and ATF-6. In resting cells, all three ER stress receptors are maintained in an inactive state, but when unfolded proteins are accumulated, they are dissociated leading to their activation and triggering the UPR. The UPR is a pro-survival response to reduce the accumulation of unfolded proteins and restore normal ER functioning. However, if protein aggregation is persistent and the stress cannot be resolved, signaling switches from pro-survival to pro-apoptotic. In our model we observed increased PERK activation with aging and $A\beta_{1-42}$ oligomers treatment that is significant in the older treated experimental group. Moreover, PERK activation leads to the significant increase of phosphorylation of eIF2α in the 18Aβ group. These results agree to others studies which have shown that PERK activation and consequent elevation of p-eIF2α attenuates general translation and, on the other hand, promotes the synthesis of ATF-4 and BACE1 resulting in the generation of Aβ with high
ability to form toxic senile plaques in AD brains. Moreover, excessive, long-term stress conditions may contribute to inducing neuronal death by apoptosis as a result of the overactivated expression of pro-apoptotic proteins via ATF-4. In this view, dysregulated translation, increased levels of p-eIF2α, may be a major contributor to structural and functional neuronal loss resulting in memory impairment[178].

The most conserved UPR signaling branch is initiated by the ER stress transducer IRE1α which is a dual-activity enzyme, having a serine–threonine kinase domain and an endoribonuclease domain that under ER stress conditions auto-phosphorylates and homodimerizes, inducing a conformational change in the cytosolic region that activates its RNase domain. IRE1α leads to the expression of XBP1s, a potent transcription factor that transactivates a cluster of UPR-target genes and, finally, provides a negative feedback loop which inhibits PERK activation to terminate UPR[179]. At this point, if the UPR has been successful, the ER returns to normal functioning and the cell survives; however, if the stress persists, it might allow the synthesis of pro-apoptotic proteins. According to Duran-Aniotz et al. that have shown the direct association between IRE1α levels and AD severity in human brain, our results underline a progressive increase in protein levels which become significant in both 18Vh and 18Aβ groups. Although during aging IRE1α decrease due to the deterioration of the UPR, probably the persisting cellular stress, also related to the decreasing GSH levels, determines the activation of IRE1α and promotes cell death and inflammation[180].

ATF-6, the third axes of UPR, is a type II transmembrane protein that remains inactive in unstressed cells. Under conditions of ER stress, activated ATF-6 moves to the nucleus from cytoplasm and induces the transcription of ER chaperones[151]. Several recent studies have demonstrated that ATF-6 counteracts the accumulation of senile plaques and its inactivation is associated with progression of AD due to the inability of neurons to survive to ER stress[151,181]. According to these considerations, our results show a significant decrease in ATF-6 levels in young and aged mice treated with $A\beta_{1-42}$ oligomers, but not in age-matched healthy mice. The ATF-6 is the least studied branch of the UPR in the context of aging. Recent evidence in nematodes suggests that the relationship between the ATF-6 and age is more complex. Burkewitz et al. demonstrated in C. elegans that ATF-6 signaling can prove detrimental with age under basal conditions, independent of its canonical UPR role in maintaining proteostasis[182].

Increasing evidence suggests that the PI3K/Akt pathway is involved in ER stress. Interestingly, the increased activation of Akt has been reported in the postmortem brains (neurons as well as glial cells) of AD patients[183]. On the contrary, Hosoi et al. demonstrated the dual regulation of Akt that appears to be activated on short-term exposure to ER stress but down-regulated on long-term exposure to ER stress[184]. Similarly, our results show a significant decrease in Akt activation, through its phosphorylation, in both aged experimental groups. Down-regulation of Akt leads to up-regulation of GSK3β in the hippocampus of AD patients and it is associated with phosphorylated Tau and NFTs[185]. GSK3β has also been reported to stimulate Aβ production whereas its pharmacological inhibition or knockdown reduces processing of APP to Aβ[186]. Consistently, GSK3β over-activation can increase the activity of PS1 and the expression of BACE1, the resulting increase of Aβ activates GSK3β, which triggers Aβ production, resulting in a positive-feedback loop[187]. On the contrary, inhibition of GSK3β reduces Aβ levels, tau hyperphosphorylation, and cognitive deficits in mice[188]. GSK3β can activate NF-κB signaling and enhance inflammation and is also a protein target for PERK[189]. In our result the activation of PERK may be responsible for GSK3β significant expression in aged mice, indeed the phosphorylation on Ser9/21 correspond to the inhibition of the kinase of interest.

Under ER stress, the UPR acts to restore protein homeostasis also through the activation of ERK, a member of the mitogen-activated protein kinases superfamily of signaling pathways, associated with the regulation of proliferation and differentiation as well as cell survival. In the CNS, ERK has a fundamental role in neuroplasticity and its

phosphorylation is induced by the binding of neurotrophins to their specific tyrosine kinase receptors or by neuronal activity leading to glutamate release and binding to its ionotropic and metabotropic receptors[190]. ERK shows stage-dependent abnormalities in mRNA and protein expression in AD and AD models[191]. Although transient ERK activation plays important roles in memory-related processes, persistent activation can lead to cell death[192]. Therefore, either hyper- or hypoactivation of ERK could contribute to disease pathways. Indeed, Webster et al. reported that in early AD is possible to observe an extensive activation of ERK, while in later stage phosphorylation, which mediate the activation, is reduced showing a strong inverse correlation with Braak stage and the Blessed score for cognition[191]. The importance of ERK on dendrites and memory impairment is consistent with the hypothesis that ERK hypoactivation in AD contributes to cognitive decline. Moreover, several studies have shown that $A\beta_{25-35}$ i.c.v. injection can inhibit ERK[193]. Different Aβ aggregates may have different effects, for example fibrillar Aβ is able to stimulate ERK, while low soluble oligomers initially stimulated but then down-regulated ERK in hippocampal slice cultures[194]. Similarly, in our model, the sustained activation of UPR determines a significant reduction in ERK activation both in healthy and lesioned old mice, showing the degradation of the neurotrophic activity also in aging.

The bioinformatic analysis conducted highlighted 68 genes significantly dysregulated in all the comparisons investigated and in the analysis with Gorilla. Among them, Mapkapk5 it has been considered for further investigation. The RNA-sequencing analysis showed the progressive decrease in gene expression from healthy young mice to old lesioned experimental group and its decline appears to be related to aging and $A\beta_{1-42}$ treatment. Mapkapk5, is a serine/threonine protein kinase activated through a direct MAPK-dependent pathway to initiate and regulate diverse cellular processes, such as proliferation, differentiation, apoptosis and gene expression, in response to various external stimuli[195,196]. Improper signaling or dysregulation of the cascades regulated by various MAPK enzymes can induce the development or progress of different diseases, such as cancers, diabetes, or developmental disorders. A link between AD and reduced levels of Mapkapk5 has been already proposed[197]. Our results have shown a significant decrease in Mapkapk5 gene expression with the progression of the pathology. Although protein levels evaluation did not show a significant decrease, it was possible to observe a trend in this direction.

6. CONCLUSIONS

Dementia is one of the 21st century's most significant public health issues, largely due to the dramatic lifespan increase. AD is the most frequent type of dementia that begins with brain changes many years before clinical symptoms appear. This multifaceted disease is characterized by Aβ accumulation in amyloid plaques, tau aggregation in NFT, brain atrophy caused by loss of neurons and synapses, and neuroinflammation. Although AD progression is closely linked to Aβ aggregation, years of research suggest that several other factors are likely related to AD development and progression. Indeed, the loss of cholinergic transmission, progressive oxidative damage, excitotoxicity, and neuroinflammatory processes play a pivotal role in AD.

To date, there is no cure for AD, and drugs available are only symptomatic and ineffective with the progression of disease, when mostly neurons are dead or compromised. There is an urgent need to find early predictors of the disease, especially for the sporadic cases, to have more chances to start early treatments and neuroprotective strategies to give years with high quality life to patients. It is likely reasonable to argue that complex multifactorial diseases, such as AD, cannot be efficiently treated by modulating a single target, but they will require multitarget drug treatment to address the different pathological side of this disease.

The present study has been focused on the role of the aging process and UPR in AD onset through an integrate approach of bioinformatics, behavioral, and biomolecular analysis in a murine model of AD induced by i.c.v. injection of $A\beta_{1-42}$ oligomers. Although several aspects are shared in AD and aging neurodegenerative process, the results presented in this study underline the efficacy of a mouse model able to produce cognitive dysfunction in few weeks, and allow

the identification of a target, Mapkapk5, significantly dysregulated in the comparisons performed. In conclusion the study provides a better understanding of AD's pathophysiology and UPR involvement. Further studies need to be addressed to better understand how new therapeutic approaches able to enhance Mapkapk5 levels may interfere and modulate AD evolution.

7. BIBLIOGRAPHY

1. Solanki, I., Parihar, P. & Parihar, M. S. Neurodegenerative diseases: From available treatments to prospective herbal therapy. *Neurochem Int* **95**, 100–108 (2016).
2. Deuschl, G. *et al.* The burden of neurological diseases in Europe: an analysis for the Global Burden of Disease Study 2017. *Lancet Public Health* **5**, e551–e567 (2020).
3. Soria Lopez, J. A., González, H. M. & Léger, G. C. Alzheimer's disease. *Handb Clin Neurol* **167**, 231–255 (2019).
4. Braak, H., Thal, D. R., Ghebremedhin, E. & Del Tredici, K. Stages of the pathologic process in Alzheimer disease: age categories from 1 to 100 years. *J Neuropathol Exp Neurol* **70**, 960–969 (2011).
5. Jack, C. R. *et al.* Tracking pathophysiological processes in Alzheimer's disease: an updated hypothetical model of dynamic biomarkers. *Lancet Neurol* **12**, 207–216 (2013).
6. Li, Q., Wu, Y., Chen, J., Xuan, A. & Wang, X. Microglia and immunotherapy in Alzheimer's disease. *Acta Neurol Scand* **145**, 273–278 (2022).
7. Scheltens, P. *et al.* Alzheimer's disease. *Lancet* **388**, 505–517 (2016).
8. 2021 Alzheimer's disease facts and figures. *Alzheimer's & Dementia* alz.12328-alz.12328 (2021) doi:10.1002/alz.12328.
9. Harada, C. N., Natelson Love, M. C. & Triebel, K. L. Normal cognitive aging. *Clin Geriatr Med* **29**, 737–752 (2013).
10. Marasco, R. A. Current and evolving treatment strategies for the Alzheimer disease continuum. *Am J Manag Care* **26**, S167–S176 (2020).
11. Cummings, J. *et al.* Alzheimer's disease drug development pipeline: 2022. *Alzheimer's & Dementia: Translational Research & Clinical Interventions* **8**, e12295 (2022).
12. Bradfield, N. I. *et al.* Baseline Amnestic Severity Predicts Progression From Amnestic Mild Cognitive Impairment to Alzheimer Disease Dementia at 3 Years. *Alzheimer Dis Assoc Disord* **32**, 190–196 (2018).
13. International, A. D. & Patterson, C. World Alzheimer Report 2018: The state of the art of dementia research: New frontiers. (2018).
14. Niu, H., Álvarez-Álvarez, I., Guillén-Grima, F. & Aguinaga-Ontoso, I. Prevalence and incidence of Alzheimer's disease in Europe: A meta-analysis. *Neurologia* **32**, 523–532 (2017).
15. Xu, J. Mortality in the United States, 2018. 8 (2020).
16. Freedman, V. A., Kasper, J. D., Spillman, B. C. & Plassman, B. L. Short-Term Changes in the Prevalence of Probable Dementia: An Analysis of the 2011-2015 National Health and Aging Trends Study. *J Gerontol B Psychol Sci Soc Sci* **73**, S48–S56 (2018).
17. Wu, Y.-T. *et al.* The changing prevalence and incidence of dementia over time - current evidence. *Nat Rev Neurol* **13**, 327–339 (2017).
18. Matthews, F. E. *et al.* A two decade dementia incidence comparison from the Cognitive Function and Ageing Studies I and II. *Nat Commun* **7**, 11398 (2016).
19. Cerasuolo, J. O. *et al.* Population-based stroke and dementia incidence trends: Age and sex variations. *Alzheimers Dement* **13**, 1081–1088 (2017).
20. World Alzheimer Report 2015, The Global Impact of Dementia: An analysis of prevalence, incidence, cost and trends. 87.
21. GBD 2016 Dementia Collaborators. Global, regional, and national burden of Alzheimer's disease and other dementias, 1990-2016: a systematic analysis for the Global Burden of Disease Study 2016. *Lancet Neurol* **18**, 88–106 (2019).

22. Zhang, X.-X. *et al.* The Epidemiology of Alzheimer's Disease Modifiable Risk Factors and Prevention. *J Prev Alzheimers Dis* **8**, 313–321 (2021).
23. Kang, S., Lee, Y. H. & Lee, J. E. Metabolism-Centric Overview of the Pathogenesis of Alzheimer's Disease. *Yonsei Med J* **58**, 479–488 (2017).
24. Hardy, J. & Selkoe, D. J. The amyloid hypothesis of Alzheimer's disease: progress and problems on the road to therapeutics. *Science (New York, N.Y.)* **297**, 353–6 (2002).
25. Müller, U. C., Deller, T. & Korte, M. Not just amyloid: physiological functions of the amyloid precursor protein family. *Nature Reviews Neuroscience* **18**, 281–298 (2017).
26. Gupta, A. & Goyal, R. Amyloid beta plaque: a culprit for neurodegeneration. *Acta Neurol Belg* **116**, 445–450 (2016).
27. Silva, M. V. F. *et al.* Alzheimer's disease: risk factors and potentially protective measures. *J Biomed Sci* **26**, 33 (2019).
28. Martorana, A. *et al.* Cerebrospinal Fluid Aβ42 Levels: When Physiological Become Pathological State. *CNS Neurosci Ther* **21**, 921–925 (2015).
29. Zhang, H., Ma, Q., Zhang, Y.-W. & Xu, H. Proteolytic processing of Alzheimer's β-amyloid precursor protein. *J Neurochem* **120 Suppl 1**, 9–21 (2012).
30. Lee, S. J. C., Nam, E., Lee, H. J., Savelieff, M. G. & Lim, M. H. Towards an understanding of amyloid-β oligomers: characterization, toxicity mechanisms, and inhibitors. *Chem Soc Rev* **46**, 310–323 (2017).
31. Walsh, D. M. *et al.* Naturally secreted oligomers of amyloid beta protein potently inhibit hippocampal long-term potentiation in vivo. *Nature* **416**, 535–9 (2002).
32. Alberdi, E. *et al.* Ca(2+) -dependent endoplasmic reticulum stress correlates with astrogliosis in oligomeric amyloid β-treated astrocytes and in a model of Alzheimer's disease. *Aging Cell* **12**, 292–302 (2013).
33. Mattson, M. P. Pathways towards and away from Alzheimer's disease. *Nature* **430**, 631–639 (2004).
34. Kumar, V. *et al.* Protein aggregation and neurodegenerative diseases: From theory to therapy. *Eur J Med Chem* **124**, 1105–1120 (2016).
35. Wang, J.-Z., Xia, Y.-Y., Grundke-Iqbal, I. & Iqbal, K. Abnormal hyperphosphorylation of tau: sites, regulation, and molecular mechanism of neurofibrillary degeneration. *J Alzheimers Dis* **33 Suppl 1**, S123-139 (2013).
36. Khan, S. S. & Bloom, G. S. Tau: The Center of a Signaling Nexus in Alzheimer's Disease. *Front Neurosci* **10**, 31 (2016).
37. Blurton-Jones, M. & Laferla, F. M. Pathways by which Abeta facilitates tau pathology. *Curr Alzheimer Res* **3**, 437–448 (2006).
38. Näslund J *et al.* Correlation between elevated levels of amyloid beta-peptide in the brain and cognitive decline. *JAMA* **283**, (2000).
39. Blennow, K. & Hampel, H. CSF markers for incipient Alzheimer's disease. *Lancet Neurol* **2**, 605–613 (2003).
40. Livingston, G. *et al.* Dementia prevention, intervention, and care: 2020 report of the Lancet Commission. *Lancet* **396**, 413–446 (2020).
41. Puzzo, D., Gulisano, W., Palmeri, A. & Arancio, O. Rodent models for Alzheimer's disease drug discovery. *Expert Opin Drug Discov* **10**, 703–711 (2015).
42. Morroni, F., Sita, G., Tarozzi, A., Rimondini, R. & Hrelia, P. Early effects of Aβ1-42 oligomers injection in mice: Involvement of PI3K/Akt/GSK3 and MAPK/ERK1/2 pathways. *Behav Brain Res* **314**, 106–115 (2016).
43. Calvo-Flores Guzmán, B. *et al.* The Interplay Between Beta-Amyloid 1–42 (Aβ1–42)-Induced Hippocampal Inflammatory Response, p-tau, Vascular Pathology, and

Their Synergistic Contributions to Neuronal Death and Behavioral Deficits. *Front Mol Neurosci* **13**, 522073 (2020).
44. Selkoe, D. J., Abraham, C. R., Podlisny, M. B. & Duffy, L. K. Isolation of Low-Molecular-Weight Proteins from Amyloid Plaque Fibers in Alzheimer's Disease. *Journal of Neurochemistry* **46**, 1820–1834 (1986).
45. Ballard, C. *et al.* Alzheimer's disease. *Lancet* **377**, 1019–1031 (2011).
46. Calero, M. *et al.* Additional mechanisms conferring genetic susceptibility to Alzheimer's disease. *Front Cell Neurosci* **9**, 138 (2015).
47. Bekris, L. M., Yu, C.-E., Bird, T. D. & Tsuang, D. W. Genetics of Alzheimer disease. *J Geriatr Psychiatry Neurol* **23**, 213–227 (2010).
48. Wolfe, M. S. Processive proteolysis by γ-secretase and the mechanism of Alzheimer's disease. *Biol Chem* **393**, 899–905 (2012).
49. Francis, Y. I., Stephanou, A. & Latchman, D. S. CREB-binding protein activation by presenilin 1 but not by its M146L mutant. *Neuroreport* **17**, 917–921 (2006).
50. Barthet, G. *et al.* Presenilin mediates neuroprotective functions of ephrinB and brain-derived neurotrophic factor and regulates ligand-induced internalization and metabolism of EphB2 and TrkB receptors. *Neurobiol Aging* **34**, 499–510 (2013).
51. Steiner, H., Capell, A., Leimer, U. & Haass, C. Genes and mechanisms involved in beta-amyloid generation and Alzheimer's disease. *Eur Arch Psychiatry Clin Neurosci* **249**, 266–270 (1999).
52. Zatti, G. *et al.* Presenilin mutations linked to familial Alzheimer's disease reduce endoplasmic reticulum and Golgi apparatus calcium levels. *Cell Calcium* **39**, 539–550 (2006).
53. Abeysinghe, A. a. D. T., Deshapriya, R. D. U. S. & Udawatte, C. Alzheimer's disease; a review of the pathophysiological basis and therapeutic interventions. *Life Sci* **256**, 117996 (2020).
54. Zhao, J., Liu, X., Xia, W., Zhang, Y. & Wang, C. Targeting Amyloidogenic Processing of APP in Alzheimer's Disease. *Front Mol Neurosci* **13**, 137 (2020).
55. Kim, J., Basak, J. M. & Holtzman, D. M. The role of apolipoprotein E in Alzheimer's disease. *Neuron* **63**, 287–303 (2009).
56. Breijyeh, Z. & Karaman, R. Comprehensive Review on Alzheimer's Disease: Causes and Treatment. *Molecules* **25**, E5789 (2020).
57. Leduc, V., Jasmin-Bélanger, S. & Poirier, J. APOE and cholesterol homeostasis in Alzheimer's disease. *Trends Mol Med* **16**, 469–477 (2010).
58. Mahley, R. W. Apolipoprotein E: from cardiovascular disease to neurodegenerative disorders. *J Mol Med (Berl)* **94**, 739–746 (2016).
59. Foster, E. M., Dangla-Valls, A., Lovestone, S., Ribe, E. M. & Buckley, N. J. Clusterin in Alzheimer's Disease: Mechanisms, Genetics, and Lessons From Other Pathologies. *Front Neurosci* **13**, 164 (2019).
60. Hersi, M. *et al.* Risk factors associated with the onset and progression of Alzheimer's disease: A systematic review of the evidence. *Neurotoxicology* **61**, 143–187 (2017).
61. Solomon, A. *et al.* Advances in the prevention of Alzheimer's disease and dementia. *J Intern Med* **275**, 229–250 (2014).
62. Herrup, K. Reimagining Alzheimer's disease--an age-based hypothesis. *J Neurosci* **30**, 16755–16762 (2010).
63. Armstrong, R.A. Risk factors for Alzheimer's disease. *Folia Neuropathol* **57**, 87–105 (2019).
64. Rossor M & Mountjoy Cq. Post-mortem neurochemical changes in Alzheimer's disease compared with normal ageing. *The Canadian journal of neurological sciences. Le journal canadien des sciences neurologiques* **13**, (1986).

65. Mortimer, J. A., French, L. R., Hutton, J. T. & Schuman, L. M. Head injury as a risk factor for Alzheimer's disease. *Neurology* **35**, 264–267 (1985).
66. Mackay, D. F. *et al.* Neurodegenerative Disease Mortality among Former Professional Soccer Players. *N Engl J Med* **381**, 1801–1808 (2019).
67. McKenzie, J. E., Gentleman, S. M., Roberts, G. W., Graham, D. I. & Royston, M. C. Increased numbers of beta APP-immunoreactive neurones in the entorhinal cortex after head injury. *Neuroreport* **6**, 161–164 (1994).
68. Redelmeier Da, Manzoor F, & Thiruchelvam D. Association Between Statin Use and Risk of Dementia After a Concussion. *JAMA neurology* **76**, (2019).
69. Skoog, I. & Gustafson, D. Update on hypertension and Alzheimer's disease. *Neurol Res* **28**, 605–611 (2006).
70. Liu, W., Wong, A., Law, A. C. K. & Mok, V. C. T. Cerebrovascular disease, amyloid plaques, and dementia. *Stroke* **46**, 1402–1407 (2015).
71. Zlokovic, B. V. Neurovascular pathways to neurodegeneration in Alzheimer's disease and other disorders. *Nat Rev Neurosci* **12**, 723–738 (2011).
72. Li, X., Song, D. & Leng, S. X. Link between type 2 diabetes and Alzheimer's disease: from epidemiology to mechanism and treatment. *Clin Interv Aging* **10**, 549–560 (2015).
73. Kimura, N. Diabetes Mellitus Induces Alzheimer's Disease Pathology: Histopathological Evidence from Animal Models. *Int J Mol Sci* **17**, 503 (2016).
74. McIntosh, T. K. *et al.* Neuropathological sequelae of traumatic brain injury: relationship to neurochemical and biomechanical mechanisms. *Laboratory investigation; a journal of technical methods and pathology* **74**, 315–42 (1996).
75. Durazzo, T. C., Mattsson, N., Weiner, M. W., & Alzheimer's Disease Neuroimaging Initiative. Smoking and increased Alzheimer's disease risk: a review of potential mechanisms. *Alzheimers Dement* **10**, S122-145 (2014).
76. Xia, X., Jiang, Q., McDermott, J. & Han, J. J. Aging and Alzheimer's disease: Comparison and associations from molecular to system level. *Aging Cell* **17**, e12802 (2018).
77. DiSabato, D. J., Quan, N. & Godbout, J. P. Neuroinflammation: the devil is in the details. *J Neurochem* **139 Suppl 2**, 136–153 (2016).
78. Lyman, M., Lloyd, D. G., Ji, X., Vizcaychipi, M. P. & Ma, D. Neuroinflammation: the role and consequences. *Neuroscience research* **79**, 1–12 (2014).
79. Heneka, M. T. *et al.* Neuroinflammation in Alzheimer's disease. *The Lancet Neurology* **14**, 388–405 (2015).
80. Wake, H., Moorhouse, A. J., Miyamoto, A. & Nabekura, J. Microglia: actively surveying and shaping neuronal circuit structure and function. *Trends Neurosci* **36**, 209–217 (2013).
81. Edler, M. K., Mhatre-Winters, I. & Richardson, J. R. Microglia in Aging and Alzheimer's Disease: A Comparative Species Review. *Cells* **10**, 1138 (2021).
82. Nimmerjahn, A., Kirchhoff, F. & Helmchen, F. Resting microglial cells are highly dynamic surveillants of brain parenchyma in vivo. *Science* **308**, 1314–1318 (2005).
83. Paolicelli, R. C. *et al.* Microglia states and nomenclature: A field at its crossroads. *Neuron* **110**, 3458–3483 (2022).
84. Hickman, S. E. *et al.* The microglial sensome revealed by direct RNA sequencing. *Nat Neurosci* **16**, 1896–1905 (2013).
85. Perry, V. H. & Holmes, C. Microglial priming in neurodegenerative disease. *Nat Rev Neurol* **10**, 217–224 (2014).
86. Mazaheri, F. *et al.* TREM2 deficiency impairs chemotaxis and microglial responses to neuronal injury. *EMBO Rep* **18**, 1186–1198 (2017).

87. Silvin, A. *et al.* Dual ontogeny of disease-associated microglia and disease inflammatory macrophages in aging and neurodegeneration. *Immunity* **55**, (2022).
88. Krasemann, S. *et al.* The TREM2-APOE Pathway Drives the Transcriptional Phenotype of Dysfunctional Microglia in Neurodegenerative Diseases. *Immunity* **47**, 566-581.e9 (2017).
89. Sobue, A. *et al.* Microglial gene signature reveals loss of homeostatic microglia associated with neurodegeneration of Alzheimer's disease. *Acta Neuropathol Commun* **9**, 1 (2021).
90. Meraz-Ríos, M. A., Toral-Rios, D., Franco-Bocanegra, D., Villeda-Hernández, J. & Campos-Peña, V. Inflammatory process in Alzheimer's Disease. *Front Integr Neurosci* **7**, 59 (2013).
91. Marlatt, M. W. *et al.* Proliferation in the Alzheimer hippocampus is due to microglia, not astroglia, and occurs at sites of amyloid deposition. *Neural Plast* **2014**, 693851 (2014).
92. Hickman, S. E., Allison, E. K. & El Khoury, J. Microglial dysfunction and defective β-amyloid clearance pathways in aging alzheimer's disease mice. *Journal of Neuroscience* **28**, 8354–8360 (2008).
93. Preman, P., Alfonso-Triguero, M., Alberdi, E., Verkhratsky, A. & Arranz, A. M. Astrocytes in Alzheimer's Disease: Pathological Significance and Molecular Pathways. *Cells* **10**, 540 (2021).
94. Sheeler, C. *et al.* Glia in Neurodegeneration: The Housekeeper, the Defender and the Perpetrator. *Int J Mol Sci* **21**, 9188 (2020).
95. García-Matas, S. *et al.* Dysfunction of astrocytes in senescence-accelerated mice SAMP8 reduces their neuroprotective capacity. *Aging Cell* **7**, 630–640 (2008).
96. Bhat, R. *et al.* Astrocyte senescence as a component of Alzheimer's disease. *PLoS One* **7**, e45069 (2012).
97. Bitto, A. *et al.* Stress-induced senescence in human and rodent astrocytes. *Exp Cell Res* **316**, 2961–2968 (2010).
98. Fischer, R. & Maier, O. Interrelation of oxidative stress and inflammation in neurodegenerative disease: role of TNF. *Oxid Med Cell Longev* **2015**, 610813 (2015).
99. Liguori, I. *et al.* Oxidative stress, aging, and diseases. *Clinical interventions in aging* **13**, 757–772 (2018).
100. Baierle, M., Nascimento, S., Moro, A. & Al., E. Relationship between inflammation and oxidative stress and cognitive decline in the institutionalized elderly. *Oxid Med Cell Longev* **2015**, (2015).
101. De la Fuente, M. & Miquel, J. An update of the oxidation-inflammation theory of aging: the involvement of the immune system in oxi-inflamm-aging. *Curr Pharm Des* **15**, 3003–26 (2009).
102. Mecocci, P. *et al.* A Long Journey into Aging, Brain Aging, and Alzheimer's Disease Following the Oxidative Stress Tracks. *Journal of Alzheimer's Disease* **62**, 1319–1335 (2018).
103. Trachootham, D. *et al.* Selective killing of oncogenically transformed cells through a ROS-mediated mechanism by beta-phenylethyl isothiocyanate. *Cancer cell* **10**, 241–252 (2006).
104. Perrig, W. J., Perrig, P. & Stähelin, H. B. The relation between antioxidants and memory performance in the old and very old. *J Am Geriatr Soc* **45**, 718–724 (1997).
105. Harman, D. Free radical theory of aging. *Mutation Research/DNAging* **275**, 257–266 (1992).
106. Butterfield, D. A. & Halliwell, B. Oxidative stress, dysfunctional glucose metabolism and Alzheimer disease. *Nat Rev Neurosci* **20**, 148–160 (2019).

107. Bonda, D. J. *et al.* Neuronal failure in Alzheimer's disease: a view through the oxidative stress looking-glass. *Neurosci. Bull.* **30**, 243–252 (2014).
108. Nunomura, A. *et al.* Oxidative damage is the earliest event in Alzheimer disease. *J Neuropathol Exp Neurol* **60**, 759–767 (2001).
109. Swerdlow, R. H. Alzheimer's Disease Pathologic Cascades: Who Comes First, What Drives What. *Neurotox Res* **22**, 182–194 (2012).
110. Zhu, X. *et al.* Activation of p38 kinase links tau phosphorylation, oxidative stress, and cell cycle-related events in Alzheimer disease. *J Neuropathol Exp Neurol* **59**, 880–888 (2000).
111. Gella, A. & Durany, N. Oxidative stress in Alzheimer disease. *Cell Adh Migr* **3**, 88–93 (2009).
112. Mattson, M. P., Carney, J. W. & Butterfield, D. A. A tombstone in Alzheimer's? *Nature* **373**, 481 (1995).
113. Münch, G., Westcott, B., Menini, T. & Gugliucci, A. Advanced glycation endproducts and their pathogenic roles in neurological disorders. *Amino Acids* **42**, 1221–1236 (2012).
114. Braakman, I. & Hebert, D. N. Protein folding in the endoplasmic reticulum. *Cold Spring Harb Perspect Biol* **5**, a013201 (2013).
115. Schwarz, D. S. & Blower, M. D. The endoplasmic reticulum: structure, function and response to cellular signaling. *Cell Mol Life Sci* **73**, 79–94 (2016).
116. English, A. R. & Voeltz, G. K. Endoplasmic reticulum structure and interconnections with other organelles. *Cold Spring Harb Perspect Biol* **5**, a013227 (2013).
117. Shibata, Y. *et al.* Mechanisms determining the morphology of the peripheral ER. *Cell* **143**, 774–788 (2010).
118. Kaushik, S. & Cuervo, A. M. Proteostasis and aging. *Nat Med* **21**, 1406–1415 (2015).
119. Hartl, F. U. & Hayer-Hartl, M. Converging concepts of protein folding in vitro and in vivo. *Nat Struct Mol Biol* **16**, 574–581 (2009).
120. Ruggiano, A., Foresti, O. & Carvalho, P. Quality control: ER-associated degradation: protein quality control and beyond. *J Cell Biol* **204**, 869–879 (2014).
121. Uddin, M. S. *et al.* Molecular Mechanisms of ER Stress and UPR in the Pathogenesis of Alzheimer's Disease. *Mol Neurobiol* **57**, 2902–2919 (2020).
122. Walter, P. & Ron, D. The unfolded protein response: from stress pathway to homeostatic regulation. *Science* **334**, 1081–1086 (2011).
123. Chow, C. Y., Wang, X., Riccardi, D., Wolfner, M. F. & Clark, A. G. The genetic architecture of the genome-wide transcriptional response to ER stress in the mouse. *PLoS Genet* **11**, e1004924 (2015).
124. Schuck, S., Prinz, W. A., Thorn, K. S., Voss, C. & Walter, P. Membrane expansion alleviates endoplasmic reticulum stress independently of the unfolded protein response. *J Cell Biol* **187**, 525–536 (2009).
125. Hetz, C., Chevet, E. & Oakes, S. A. Proteostasis control by the unfolded protein response. *Nat Cell Biol* **17**, 829–838 (2015).
126. Maurel, M., Chevet, E., Tavernier, J. & Gerlo, S. Getting RIDD of RNA: IRE1 in cell fate regulation. *Trends Biochem Sci* **39**, 245–254 (2014).
127. Ron, D. & Hubbard, S. R. How IRE1 reacts to ER stress. *Cell* **132**, 24–26 (2008).
128. Hollien, J. *et al.* Regulated Ire1-dependent decay of messenger RNAs in mammalian cells. *J Cell Biol* **186**, 323–331 (2009).

129. Hu, H., Tian, M., Ding, C. & Yu, S. The C/EBP Homologous Protein (CHOP) Transcription Factor Functions in Endoplasmic Reticulum Stress-Induced Apoptosis and Microbial Infection. *Front Immunol* **9**, 3083 (2018).
130. Wu, J. *et al.* ATF6alpha optimizes long-term endoplasmic reticulum function to protect cells from chronic stress. *Dev Cell* **13**, 351–364 (2007).
131. Soto, C. Unfolding the role of protein misfolding in neurodegenerative diseases. *Nat Rev Neurosci* **4**, 49–60 (2003).
132. Martínez, G., Duran-Aniotz, C., Cabral-Miranda, F., Vivar, J. P. & Hetz, C. Endoplasmic reticulum proteostasis impairment in aging. *Aging Cell* **16**, 615–623 (2017).
133. Ashraf, G. M. *et al.* Protein misfolding and aggregation in Alzheimer's disease and type 2 diabetes mellitus. *CNS Neurol Disord Drug Targets* **13**, 1280–1293 (2014).
134. Wang, M. & Kaufman, R. J. Protein misfolding in the endoplasmic reticulum as a conduit to human disease. *Nature* **529**, 326–335 (2016).
135. Hughes, D. & Mallucci, G. R. The unfolded protein response in neurodegenerative disorders - therapeutic modulation of the PERK pathway. *FEBS J* **286**, 342–355 (2019).
136. Gouras, G. K. *et al.* Intraneuronal Abeta42 accumulation in human brain. *Am J Pathol* **156**, 15–20 (2000).
137. Mattsson, N. *et al.* Plasma tau in Alzheimer disease. *Neurology* **87**, 1827–1835 (2016).
138. Abisambra, J. F. *et al.* Tau accumulation activates the unfolded protein response by impairing endoplasmic reticulum-associated degradation. *J Neurosci* **33**, 9498–9507 (2013).
139. Hoozemans, J. J. M. *et al.* The unfolded protein response is activated in pretangle neurons in Alzheimer's disease hippocampus. *Am J Pathol* **174**, 1241–1251 (2009).
140. Duran-Aniotz, C. *et al.* IRE1 signaling exacerbates Alzheimer's disease pathogenesis. *Acta Neuropathol* **134**, 489–506 (2017).
141. Zhao, L. & Ackerman, S. L. Endoplasmic reticulum stress in health and disease. *Curr Opin Cell Biol* **18**, 444–452 (2006).
142. Cai, Y. *et al.* Interplay of endoplasmic reticulum stress and autophagy in neurodegenerative disorders. *Autophagy* **12**, 225–244 (2016).
143. Fujikake, N., Shin, M. & Shimizu, S. Association Between Autophagy and Neurodegenerative Diseases. *Front Neurosci* **12**, 255 (2018).
144. Sharma, V. *et al.* Local Inhibition of PERK Enhances Memory and Reverses Age-Related Deterioration of Cognitive and Neuronal Properties. *J Neurosci* **38**, 648–658 (2018).
145. Devi, L. & Ohno, M. PERK mediates eIF2α phosphorylation responsible for BACE1 elevation, CREB dysfunction and neurodegeneration in a mouse model of Alzheimer's disease. *Neurobiol Aging* **35**, 2272–2281 (2014).
146. Pasini, S., Corona, C., Liu, J., Greene, L. A. & Shelanski, M. L. Specific downregulation of hippocampal ATF4 reveals a necessary role in synaptic plasticity and memory. *Cell Rep* **11**, 183–191 (2015).
147. Ma, T. *et al.* Suppression of eIF2α kinases alleviates Alzheimer's disease-related plasticity and memory deficits. *Nat Neurosci* **16**, 1299–1305 (2013).
148. Llorens-Martín, M., Jurado, J., Hernández, F. & Avila, J. GSK-3β, a pivotal kinase in Alzheimer disease. *Front Mol Neurosci* **7**, 46–46 (2014).
149. Martínez, G. *et al.* Regulation of Memory Formation by the Transcription Factor XBP1. *Cell Rep* **14**, 1382–1394 (2016).

150. Cissé, M., Duplan, E. & Checler, F. The transcription factor XBP1 in memory and cognition: Implications in Alzheimer disease. *Mol Med* **22**, 905–917 (2017).
151. Du, Y. *et al.* Activating transcription factor 6 reduces Aβ1-42 and restores memory in Alzheimer's disease model mice. *Int J Neurosci* **130**, 1015–1023 (2020).
152. Santos, L. E. & Ferreira, S. T. Crosstalk between endoplasmic reticulum stress and brain inflammation in Alzheimer's disease. *Neuropharmacology* **136**, 350–360 (2018).
153. Li, Y., Guo, Y., Tang, J., Jiang, J. & Chen, Z. New insights into the roles of CHOP-induced apoptosis in ER stress. *Acta Biochim Biophys Sin (Shanghai)* **46**, 629–640 (2014).
154. LaFerla, F. M., Green, K. N. & Oddo, S. Intracellular amyloid-beta in Alzheimer's disease. *Nat Rev Neurosci* **8**, 499–509 (2007).
155. Maezawa, I. *et al.* Congo red and thioflavin-T analogs detect Aβ oligomers. *J Neurochem* **104**, 457–468 (2008).
156. Hong, H. S. *et al.* Combining the rapid MTT formazan exocytosis assay and the MC65 protection assay led to the discovery of carbazole analogs as small molecule inhibitors of Aβ oligomer-induced cytotoxicity. *Brain Res* **1130**, 223–234 (2007).
157. Sarter, M., Bodewitz, G. & Stephens, D. N. Attenuation of scopolamine-induced impairment of spontaneous alteration behaviour by antagonist but not inverse agonist and agonist beta-carbolines. *Psychopharmacology* **94**, 491–5 (1988).
158. Lopes, I. S. *et al.* Riparin II ameliorates corticosterone-induced depressive-like behavior in mice: Role of antioxidant and neurotrophic mechanisms. *Neurochem Int* **120**, 33–42 (2018).
159. Morroni, F. *et al.* Neuroprotective effect of caffeic acid phenethyl ester in a mouse model of Alzheimer's disease involves Nrf2/HO-1 pathway. *Aging Dis* (2018) doi:10.14336/AD.2017.0903.
160. Bradford, M. M. A rapid and sensitive method for the quantitation of microgram quantities of protein utilizing the principle of protein-dye binding. *Anal Biochem* **72**, 248–54 (1976).
161. Kim, D., Langmead, B. & Salzberg, S. L. HISAT: a fast spliced aligner with low memory requirements. *Nat Methods* **12**, 357–360 (2015).
162. Pertea, M. *et al.* StringTie enables improved reconstruction of a transcriptome from RNA-seq reads. *Nat Biotechnol* **33**, 290–295 (2015).
163. Love, M. I., Huber, W. & Anders, S. Moderated estimation of fold change and dispersion for RNA-seq data with DESeq2. *Genome Biol* **15**, 550 (2014).
164. Mootha, V. K. *et al.* PGC-1alpha-responsive genes involved in oxidative phosphorylation are coordinately downregulated in human diabetes. *Nat Genet* **34**, 267–273 (2003).
165. Chen, J., Aronow, B. J. & Jegga, A. G. Disease candidate gene identification and prioritization using protein interaction networks. *BMC Bioinformatics* **10**, 73 (2009).
166. Eden, E., Navon, R., Steinfeld, I., Lipson, D. & Yakhini, Z. GOrilla: a tool for discovery and visualization of enriched GO terms in ranked gene lists. *BMC Bioinformatics* **10**, 48 (2009).
167. Mi, H. *et al.* Protocol Update for Large-scale genome and gene function analysis with PANTHER Classification System (v.14.0). *Nat Protoc* **14**, 703–721 (2019).
168. Morroni, F., Sita, G., Tarozzi, A., Cantelli-Forti, G. & Hrelia, P. Neuroprotection by 6-(methylsulfinyl)hexyl isothiocyanate in a 6-hydroxydopamine mouse model of Parkinson's disease. *Brain Research* **1589**, 93–104 (2014).
169. Chiba, T. *et al.* Amyloid-beta causes memory impairment by disturbing the JAK2/STAT3 axis in hippocampal neurons. *Mol Psychiatry* **14**, 206–222 (2009).

170. Yang, W., Zhou, X. & Ma, T. Memory Decline and Behavioral Inflexibility in Aged Mice Are Correlated With Dysregulation of Protein Synthesis Capacity. *Front Aging Neurosci* **11**, 246 (2019).
171. Leutner, S., Eckert, A. & Müller, W. E. ROS generation, lipid peroxidation and antioxidant enzyme activities in the aging brain. *J Neural Transm (Vienna)* **108**, 955–967 (2001).
172. Mandal, P. K., Saharan, S., Tripathi, M. & Murari, G. Brain Glutathione Levels – A Novel Biomarker for Mild Cognitive Impairment and Alzheimer's Disease. *Biological Psychiatry* **78**, 702–710 (2015).
173. Belrose, J. C., Xie, Y.-F., Gierszewski, L. J., MacDonald, J. F. & Jackson, M. F. Loss of glutathione homeostasis associated with neuronal senescence facilitates TRPM2 channel activation in cultured hippocampal pyramidal neurons. *Molecular Brain* **5**, 11–11 (2012).
174. Chen, T. S., Richie, J. P. & Lang, C. A. The effect of aging on glutathione and cysteine levels in different regions of the mouse brain. *Proc Soc Exp Biol Med* **190**, 399–402 (1989).
175. Viana, R. J. S., Nunes, A. F. & Rodrigues, C. M. P. Endoplasmic reticulum enrollment in Alzheimer's disease. *Mol Neurobiol* **46**, 522–534 (2012).
176. Kondo, T. *et al.* Modeling Alzheimer's disease with iPSCs reveals stress phenotypes associated with intracellular Aβ and differential drug responsiveness. *Cell Stem Cell* **12**, 487–496 (2013).
177. Duran-Aniotz, C., Martínez, G. & Hetz, C. Memory loss in Alzheimer's disease: are the alterations in the UPR network involved in the cognitive impairment? *Front Aging Neurosci* **6**, 8 (2014).
178. Rozpedek, W., Markiewicz, L., Diehl, J. A., Pytel, D. & Majsterek, I. Unfolded Protein Response and PERK Kinase as a New Therapeutic Target in the Pathogenesis of Alzheimer's Disease. *Curr Med Chem* **22**, 3169–3184 (2015).
179. Lee, A.-H., Iwakoshi, N. N. & Glimcher, L. H. XBP-1 regulates a subset of endoplasmic reticulum resident chaperone genes in the unfolded protein response. *Mol Cell Biol* **23**, 7448–7459 (2003).
180. Cabral-Miranda, F. *et al.* Control of mammalian brain aging by the unfolded protein response (UPR). 2020.04.13.039172 Preprint at https://doi.org/10.1101/2020.04.13.039172 (2020).
181. Katayama, T. *et al.* Disturbed activation of endoplasmic reticulum stress transducers by familial Alzheimer's disease-linked presenilin-1 mutations. *J Biol Chem* **276**, 43446–43454 (2001).
182. Burkewitz, K. *et al.* Atf-6 Regulates Lifespan through ER-Mitochondrial Calcium Homeostasis. *Cell Rep* **32**, 108125 (2020).
183. Griffin, R. J. *et al.* Activation of Akt/PKB, increased phosphorylation of Akt substrates and loss and altered distribution of Akt and PTEN are features of Alzheimer's disease pathology. *J Neurochem* **93**, 105–117 (2005).
184. Hosoi, T., Hyoda, K., Okuma, Y., Nomura, Y. & Ozawa, K. Akt up- and down-regulation in response to endoplasmic reticulum stress. *Brain Research* **1152**, 27–31 (2007).
185. Ferrer, I., Barrachina, M. & Puig, B. Glycogen synthase kinase-3 is associated with neuronal and glial hyperphosphorylated tau deposits in Alzheimer's disease, Pick's disease, progressive supranuclear palsy and corticobasal degeneration. *Acta Neuropathol* **104**, 583–591 (2002).
186. Wen, Y. *et al.* Interplay between cyclin-dependent kinase 5 and glycogen synthase kinase 3 beta mediated by neuregulin signaling leads to differential effects

on tau phosphorylation and amyloid precursor protein processing. *J Neurosci* **28**, 2624–2632 (2008).
187. D'Mello, S. R. When Good Kinases Go Rogue: GSK3, p38 MAPK and CDKs as Therapeutic Targets for Alzheimer's and Huntington's Disease. *International Journal of Molecular Sciences* **22**, 5911 (2021).
188. Iqbal, K., Liu, F. & Gong, C.-X. Tau and neurodegenerative disease: the story so far. *Nat Rev Neurol* **12**, 15–27 (2016).
189. Baltzis, D. *et al.* The eIF2alpha kinases PERK and PKR activate glycogen synthase kinase 3 to promote the proteasomal degradation of p53. *J Biol Chem* **282**, 31675–31687 (2007).
190. Cruz, C. D. & Cruz, F. The ERK 1 and 2 Pathway in the Nervous System: From Basic Aspects to Possible Clinical Applications in Pain and Visceral Dysfunction. *Curr Neuropharmacol* **5**, 244–252 (2007).
191. Webster, B. *et al.* Astroglial activation of extracellular-regulated kinase in early stages of Alzheimer disease. *J Neuropathol Exp Neurol* **65**, 142–151 (2006).
192. Zhuang, S. & Schnellmann, R. G. A death-promoting role for extracellular signal-regulated kinase. *J Pharmacol Exp Ther* **319**, 991–997 (2006).
193. Jin, Y. *et al.* Sodium ferulate prevents amyloid-beta-induced neurotoxicity through suppression of p38 MAPK and upregulation of ERK-1/2 and Akt/protein kinase B in rat hippocampus. *Acta Pharmacol Sin* **26**, 943–951 (2005).
194. Bell, K. A., O'Riordan, K. J., Sweatt, J. D. & Dineley, K. T. MAPK recruitment by beta-amyloid in organotypic hippocampal slice cultures depends on physical state and exposure time. *J Neurochem* **91**, 349–361 (2004).
195. Cargnello, M. & Roux, P. P. Activation and Function of the MAPKs and Their Substrates, the MAPK-Activated Protein Kinases. *Microbiology and Molecular Biology Reviews* **75**, 50–83 (2011).
196. Maroofian, R. *et al.* Consolidating the association of biallelic MAPKAPK5 pathogenic variants with a distinct syndromic neurodevelopmental disorder. *Journal of Medical Genetics* (2022) doi:10.1136/jmg-2022-108566.
197. Kiddle, S. J. *et al.* Plasma protein biomarkers of Alzheimer's disease endophenotypes in asymptomatic older twins: early cognitive decline and regional brain volumes. *Transl Psychiatry* **5**, e584 (2015).